HHS Public Access

Author manuscript

Brain Struct Funct. Author manuscript; available in PMC 2018 April 01.

Published in final edited form as:

Brain Struct Funct. 2018 April ; 223(3): 1133–1148. doi:10.1007/s00429-017-1542-8.

Perineuronal nets labeled by monoclonal antibody VC1.1 ensheath interneurons expressing parvalbumin and calbindin in the rat amygdala

Alexander J. McDonald[*,1], **Patricia G. Hamilton**[1], and **Colin J. Barnstable**[2]

[1]Department of Pharmacology, Physiology and Neuroscience, University of South Carolina School of Medicine, Columbia, SC, USA

[2]Department of Neural and Behavioral Sciences, The Pennsylvania State University College of Medicine, Hershey, PA, USA

Abstract

Perineuronal nets (PNNs) are specialized condensations of extracellular matrix that ensheath particular neuronal subpopulations in the brain and spinal cord. PNNs regulate synaptic plasticity, including the encoding of fear memories by the amygdala. The present immunohistochemical investigation studied PNN structure and distribution, as well as the neurochemistry of their ensheathed neurons, in the rat amygdala using monoclonal antibody VC1.1, which recognizes a glucuronic acid 3-sulfate glycan associated with PNNs in the cerebral cortex. VC1.1+ PNNs surrounded the cell bodies and dendrites of a subset of nonpyramidal neurons in cortex-like portions of the amygdala (basolateral amygdalar complex, cortical nuclei, nucleus of the lateral olfactory tract, and amygdalohippocampal region). There was also significant neuropilar VC1.1 immunoreactivity whose density varied in different amygdalar nuclei. Cell counts in the basolateral nucleus revealed that virtually all neurons ensheathed by VC1.1+ PNNs were parvalbumin-positive (PV+) interneurons, and these VC1.1+/PV+ cells constituted 60% of all PV+ interneurons, including all of the larger PV+ neurons. Approximately 70% of VC1.1+ neurons were calbindin-positive (CB+), and these VC1.1+/CB+ cells constituted about 40% of all CB+ neurons. Colocalization of VC1.1 with Vicia villosa agglutinin (VVA) binding, which stains terminal N-acetylgalactosamines, revealed that VC1.1+ PNNs were largely a subset of VVA+ PNNs. This investigation provides baseline data regarding PNNs in the rat which should be useful for future studies of their function in this species.

Keywords

extracellular matrix; perineuronal nets; amygdala; calcium binding proteins; immunohistochemistry

[*]**Correspondence to:** Alexander J. McDonald, Telephone: 803-216-3511, alexander.mcdonald@uscmed.sc.edu.

Ethical approval: All applicable international, national, and/or institutional guidelines for the care and use of animals were followed.

All procedures performed in studies involving animals were in accordance with the ethical standards of the institution or practice at which the studies were conducted.

Conflict of interest: The authors declare that they have no conflict of interest.

Introduction

Perineuronal nets (PNNs) are specialized condensations of extracellular matrix that ensheath the cell bodies, proximal dendrites, and axon initial segments of neurons. They were initially described by Camillo Golgi using his Golgi technique (Golgi, 1893; Celio and Blümke, 1994; Celio et al., 1998). Investigations conducted in the last 25 years have shown that PNNs consist of a variety of glycoconjugates including hyaluronic acid, proteoglycans, and glycoproteins (Galtrey and Fawcett, 2007; Berretta et al., 2015; Smith et al., 2015). Recent studies have demonstrated that PNNs are formed during postnatal development and are critical for the regulation of a variety of synaptic functions including synaptic stabilization and synaptic plasticity (Galtrey and Fawcett, 2007; Berretta et al., 2015). The finding that PNNs and other components of the extracellular matrix are altered in several neurological and neuropsychiatric diseases suggests that a greater understanding of their structure and function could lead to novel therapies to treat these disorders (Viapiano and Matthews, 2006; Galtrey and Fawcett, 2007; Berretta et al., 2015; Maeda, 2015; Smith et al., 2015; Pantazopoulos and Berretta 2016; Sorg et al., 2016).

PNNs are found throughout the central nervous system but have been most extensively studied in the cerebral cortex and cerebellum. Various components are synthesized by the ensheathed neuron and/or neighboring glial cells (Carulli et al., 2006). The backbone of PNNs consists of long hyaluronic acid molecules attached to the ensheathed neuron, to which numerous chondroitin sulfate proteoglycans (CSPGs) are bound via link proteins. These CSPGs are mainly lecticans (e.g. aggrecan and brevican), whose core proteins are attached at one end to hyaluronic acid, and at the other end to the glycoprotein tenascin-R. PNNs are of heterogeneous composition and different neuronal subpopulations can be labeled by: (1) antibodies to distinct core proteins or glycosaminoglycan (GAG) sidechains of CSPGs, (2) by lectins which bind to distinct components of the GAGs, or (3) by antibodies to other carbohydrate moieties of PNNs. The same glycoconjugates that are concentrated in PNNs are also found diffusely distributed in the neuropil where they contribute to the extracellular matrix in the extracellular space around glial cells, blood vessels and neural processes including nodes of Ranvier (Celio et al., 1998; Bekku et al., 2009).

The lectins Wisteria floribunda agglutinin (WFA) and Vicia villosa agglutinin (VVA), which bind to terminal N-acetylgalactosamines on the GAG sidechains of lecticans, are commonly used to label PNNs in the cerebral cortex and other CNS areas. A large percentage of WFA+ and VVA+ PNNs in the cortex are also labeled by antibodies that recognize a unique carbohydrate epitope that contains glucuronic acid 3-sulfate (Yamamoto et al., 1988; Barnstable et al., 1992). One of these antibodies, HNK-1, was raised against human natural killer cells (Abo and Balch, 1981), while the other, VC1.1, was generated using a homogenate of cat visual cortex (Arimatsu et al., 1987). The epitopes of HNK-1 and VC1.1 antibodies are either identical or overlapping, and are also found on N-CAM cell adhesion molecules (Kosaka et al., 1990; Naegele and Barnstable, 1991). Staining produced by these two antibodies is identical and both label PNNs ensheathing a subpopulation of neocortical GABAergic neurons that express the calcium-binding protein parvalbumin (Kosaka et al., 1990). HNK-1-positive PNNs also ensheath PV+ interneurons in the hippocampus (Ren et

al., 1994; Weber et al., 1999). Studies in the hippocampus have shown that tenascin-R molecules carrying the VC1.1/HNK-1 carbohydrate epitope modulate perisomatic inhibition and long-term potentiation (Saghatelyan et al., 2000, 2001; Bukalo et al., 2001)

Most studies of PNNs in the amygdala have been performed in human and non-human primates (Härtig et al., 1995; Pantazopoulos et al., 2006, 2008; Mueller et al., 2016). Using WFA as a marker for PNNs, Härtig and coworkers (1995) demonstrated that many neurons ensheathed by PNNs in the monkey basolateral amygdala express the calcium-binding proteins PV or calbindin (CB). Likewise Pantazopoulos and coworkers (2006) found that about one-third of PV+ interneurons in the human basolateral amygdala were ensheathed by WFA+ PNNs, and a subset of these neurons also expressed CB. The finding that there is significant loss of PNNs in the basolateral amygdala of patients with schizophrenia implicates these structures in the dysfunction of GABAergic neurons in this disorder (Pantazopoulos et al., 2010, 2015; Berretta, 2012; Berretta et al., 2015).

Much less is known about the neuroanatomy and neurochemistry of PNNs in the rodent amygdala. As in cortical structures, WFA+ PNNs develop postnatally in the rodent basolateral amygdala, increasing in number through juvenile, adolescent, and adult stages (Gogolla et al., 2009; Horii-Hayashi et al., 2015; Umemori et al., 2015; Baker et al., 2017). In a study describing the distribution and composition of PNNs throughout the rat brain, PNNs were described in the amygdala that differentially expressed aggrecan, brevican, and/or tenascin-R, but their location in individual amygdalar nuclei was not mentioned (Dauth et al., 2016). Perhaps the most remarkable finding about amygdalar PNNs to date is that it is the formation of WFA+ PNNs in the rat basolateral amygdala during postnatal days 16-21 that protects fear memories from erasure during extinction training (Gogolla et al., 2009). Likewise, it has been found that intra-amygdalar injections of chondroitinase (to deplete PNNs that express chondroitin sulfate proteoglycans) combined with extinction training erased drug-induced conditioned place preference memory (Xue et al., 2014).

These studies implicating amygdalar PNNs in synaptic plasticity and emotional learning suggest that a greater understanding of their structure, neurochemistry, cell-type-specific expression, and function in rodents could lead to novel therapies to treat anxiety disorders, drug addiction, and psychoses. Interestingly, very recent studies using WFA to stain PNNs in the rodent basolateral amygdala have shown that these N-acetylgalactosamine-positive PNNs ensheath both glutamatergic pyramidal neurons, the principal neurons of the basolateral amygdala, as well as PV+ interneurons (Baker et al., 2017; Morikawa et al., 2017). However, nothing is known about the expression of the VC1.1/HNK-1 carbohydrate epitope in the amygdala. In order to better understand the neurochemical heterogeneity of PNNs in the amygdala, we examined the structure and distribution of PNNs in the rat amygdala labeled by the VC1.1 antibody, and also analysed coexpression of N-acetylgalactosamines in these PNNs using the lectin VVA. In addition, we determined whether VC1.1+ PNNs ensheath PV+ and CB+ GABAergic interneurons in the basolateral amygdala, like they do in the cortex.

Experimental procedures

Tissue preparation

A total of 13 adult male Sprague-Dawley rats (250-350g; Envigo, Indianapolis, IN) were used in this study. All experiments were carried out in accordance with the National Institutes of Health Guide for the Care and Use of Laboratory Animals and were approved by the Institutional Animal Use and Care Committee (IACUC) of the University of South Carolina. All efforts were made to minimize animal suffering and to use the minimum number of animals necessary to produce reliable scientific data.

Rats were anesthetized with sodium pentobarbital (40 mg/kg, IP) and perfused through the heart with 0.1 M phosphate-buffered saline (PBS; pH 7.4) containing 1% sodium nitrite (100 ml), followed by mixture of 4.0% paraformaldehyde and 0.1% glutaraldehyde in 0.1 M phosphate buffer (pH 7.4; 500 ml). Following perfusion, brains were removed, postfixed in the perfusate for 3 h, and sectioned at 50 μm in the coronal plane using a vibratome. Amygdalar sections were placed in tissue culture chamber slides for immunohistochemical processing.

Single-labeling immunohistochemistry for VC1.1

Sections from five rats were processed for VC1.1 immunohistochemistry alone. The VC1.1 monoclonal antibody was produced in the Barnstable laboratory (Arimatsu et al., 1987; Barnstable et al., 1992). Sections through the amygdala were incubated in VC1.1 mouse monoclonal antibody (1:150). Following an overnight incubation in primary antibody (4°C), sections were processed for the avidin–biotin immunoperoxidase technique using a mouse IgM ABC kit (Vector Laboratories, Burlingame, CA, USA) with nickel-intensified DAB as a chromogen to produce a black reaction product (Hancock, 1986). All immunoreagents were diluted in PBS containing Triton X-100 (0.05%) and 1% normal goat serum. Following immunohistochemical processing, sections from three of the five brains were mounted on gelatinized slides, dried overnight, dehydrated in ethanols, cleared in xylene, and coverslipped with Permount (Fisher Scientific, Pittsburgh, PA, USA). Slides from the other two brains were counterstained with pyronin Y (Sigma Chemical Co., St. Louis, MO), a red Nissl stain, before dehydration in order to better appreciate the location of VC1.1-immunoreactive (VC1.1+) perineuronal nets (PNNs) in relation to the different nuclei of the amygdala. In one of the latter brains the locations of VC1.1+ PNNs in the amygdala were plotted at 0.5-mm intervals onto template drawings taken from an atlas of the rat brain (Paxinos and Watson, 1997).

Dual-labeling immunohistochemistry for VC1.1 and calcium-binding proteins

Sections from six rats were first processed for VC1.1 immunoreactivity as described above and then alternate sections were incubated in a rabbit parvalbumin (PV) antibody (1:2000) or a rabbit calbindin-D_{28k} (CB) antibody (1:50,000) (both obtained from Kenneth Baimbridge, University of British Columbia, Vancouver, Canada). Thus, half of the sections were dual labeled for VC1.1/PV and the other half for VC1.1/CB. The high dilution of the CB antibody was used to distinguish interneurons, which exhibit high levels of CB-ir, from pyramidal cells, which in many amygdalar nuclei exhibit low levels of CB-ir (McDonald and

Betette, 2001). Pyramidal cells exhibited little or no CB-ir with the dilutions used in this study. Following an overnight incubation in primary antibody (4°C), sections were processed for the avidin–biotin immunoperoxidase technique using a rabbit ABC kit (Vector Laboratories) with non-intensified DAB as a chromogen to produce a brown reaction product. All immunoreagents were diluted in PBS containing Triton X-100 (0.05%) and 1% normal goat serum. Following immunohistochemical processing, sections were mounted on gelatinized slides, dried overnight, dehydrated in ethanols, cleared in xylene, and coverslipped with Permount. Control sections processed as described above but with the PV or CB antibody omitted exhibited no brown perikaryal staining.

Colocalization of PV and VC1.1 revealed that a subset of amygdalar PV+ neurons were ensheathed by PNNs. To estimate the percentage of PV+ neurons that were ensheathed by PNNs counts of the following neuronal types in the anterior subdivision of the basolateral nucleus (BLa) were made in three of the brains stained for PV and VC1.1: (1) PV+ cell bodies ensheathed by VC1.1+ PNNs; (2) PV+ cell bodies that were not ensheathed by VC1.1+ PNNs; and (3) PV-negative cell bodies ensheathed by VC1.1+ PNNs. The BLa was chosen for this analysis since it contained the most PNNs, and because the levels of neuropilar VC1.1-ir were low, which made it easier to discriminate cell bodies ensheathed by PNNs versus those that were surrounded by high levels of neuropilar VC1.1-ir. Counts in the BLa of each of these three types of neurons were made in a total of 7-10 amygdalar sections from each brain (from both left and right sides; bregma levels −1.7 to −3.0). Analogous counts for CB and VC1.1 in the BLa were made in 8-9 amygdalar sections from each brain.

It appeared that the PV+ cell bodies that were ensheathed by VC1.1+ PNNs in the BLa were generally larger than those that were not ensheathed by PNNs. To determine if there were statistically significant morphological differences in these two types of PV+ neurons, the lengths and widths of the cell bodies of both types of neurons in the BLa were measured in two brains at 400× magnification using a calibrated ocular reticule. Cell bodies of BLa PV+ neurons were measured in a total of 11-13 amygdalae from each brain (from both left and right sides; bregma levels −1.7 to −3.0). In each section analyzed all cell bodies in the BLa that were PV+/VC1.1+ or PV+/VC1.1-negative were measured. The sum of the length and width of each cell body was used as a measure of cell body size, and the ratio of the length and width was used as an indicator of cell body shape (i.e., elongation). Both the cell body and nucleus of PV+ neurons were stained, but their nucleoli appeared as small unstained round profiles within the nucleus. Only PV+ cell bodies with a nucleolus in the section were measured in order to ensure that the cell body profile measured was near the center of the cell body rather than near the edge of the cell body where it would appear smaller. Since t-tests revealed that there was no statistically significant difference in the size and elongation data from the two brains, these data was pooled. Statistical comparisons of the cell body size and elongation data of PV+/VC1.1+ neurons and PV+/VC1.1-negative neurons were made using Student’s t-tests.

Colocalization of VC1.1-ir and VVA binding in amygdalar PNNs

The lectins Vicia villosa agglutinin (VVA) and Wisteria floribunda agglutinin (WFA), which bind to terminal N-acetylgalactosamines on the GAG sidechains of lecticans, are commonly used to label PNNs in the cerebral cortex and other CNS areas. In two rats alternate 50 μm sections through the amygdala were processed for VC1.1 immunohistochemistry or VVA histochemistry in order to compare the neuronal localization of these two PNN components. VC1.1 immunoperoxidase histochemistry was performed as described above. For VVA staining sections were incubated in HRP-conjugated VVA (40 μg/ml in PBS with 1% bovine serum albumin; E-Y Labs, Inc., San Mateo, CA) for 3.5 h at room temperature and then in nickel-intensified DAB-H_2O_2 to produce a black reaction product (Hancock, 1986). Sections that were incubated in VVA-HRP that had been preadsorbed for 1 h with N-acetylgalactosamine (0.1 M; Sigma Chemical Co., St. Louis, MO) showed no staining. In one brain the locations of VVA+ PNNs in the amygdala were plotted at 0.5-mm intervals onto template drawings taken from an atlas of the rat brain (Paxinos and Watson, 1997).

Colocalization of VC1.1 and N-acetylgalactosamine (detected by VVA-HRP) in neurons of the BLa was investigated in both brains using the mirror technique (McDonald and Betette, 2001). The use of low concentrations of Triton X-100 (0.05%) in the incubation solutions limited immunostaining to the upper and lower surfaces of the section. Profiles of all VC1.1+ cell bodies, as well as blood vessel lumina as fiducial landmarks, at one surface of each VC1.1-stained section were drawn using a camera lucida at 200× magnification. Then the corresponding surface of the adjacent VVA-stained section was viewed through the microscope and the lumina of the fiducial blood vessels were superimposed upon those of the drawing of the VC1.1-stained section (seen through the camera lucida). Profiles of all VVA+ somata at the surface of the section were then drawn. VVA+ somata that were in the same position, and of corresponding shape, as VC1.1+ somata were considered to exhibit coexistence of the two PNN components. Since almost all VC1.1+ and VVA+ dendrites were less than 3 mm wide, it was not difficult to distinguish cell bodies from dendrites.

To estimate the extent of overlap of VC1.1+ and VVA+ neurons, counts of the following neuronal types in the BLa were made in both brains: (1) double-labeled VC1.1+/VVA+ cell bodies; (2) single-labeled VC1.1+/VVA-negative cell bodies; and (3) single-labeled VVA+/VC1.1-negative cell bodies. Counts in the BLa of each of these three types of neurons were made in a total of 6-7 amygdalar sections from each brain (from both left and right sides; bregma levels −1.7 to −3.0).

Antibody Specificity

The monoclonal VC1.1 IgM antibody was generated in mice using an unfixed homogenate of cat area 17 and has been extensively characterized (Arimatsu et al., 1987; Barnstable et al., 1992). The VC1.1 antibody recognizes an N-linked carbohydrate epitope associated with integral membrane proteins that is either identical to or highly overlaps the carbohydrate epitope labeled by the HNK-1 antibody (Arimatsu et al., 1987; Kosaka et al., 1990; Naegele and Barnstable, 1991; Barnstable et al., 1992). This VC1.1/HNK-1 carbohydrate epitope has been shown to be a sulfated trisaccharide that has a unique terminal sulfated glucuronic acid (Kizuka and Oka, 2012). It is carried by several extracellular matrix components including

myelin associated glycoproteins (95-105 kDa band), N-CAMs (145 kDa and 170 kDa bands), some aggrecan proteoglycans (650-700 kDa bands), and tenascin–R (Arimatsu et al., 1987; Zaremba et al., 1990; Naegele and Barnstable, 1991; Barnstable et al., 1992; Matthews et al., 2002). In previous studies VC1.1 immunoreactivity was found in PNNs and the neuropil in the cortex, as well as in subcortical regions including the thalamic reticular nucleus. In the coronal amygdalar sections used in the present study VC1.1 immunostaining in the cortex and reticular nucleus at the level of the amygdala was identical to that obtained in previous studies (Arimatsu et al., 1987; Barnstable et al., 1992). Sections incubated with the primary antibody omitted exhibited no immunostaining.

The polyclonal PV antiserum (antiserum R-301) and CB antiserum (antiserum R-8701) were generously donated by Dr. Kenneth G. Baimbridge (University of British Columbia). The polyclonal PV antiserum was raised in rabbit against rat muscle PV. The CB antiserum was raised in rabbit against bovine cerebellar CB. Previous adsorption studies have shown that each antiserum recognizes its respective antigen, but not other calcium-binding proteins (Condé et al., 1994). Sections incubated in preimmune serum, normal rabbit serum, or PBS in place of the primary antisera exhibited no immunostaining.

Results

Single-labeling immunohistochemistry

VC1.1 immunoreactivity (VC1.1-ir) was very intense in perineuronal nets (PNNs) ensheathing the cell bodies and proximal dendrites of particular neuronal subpopulations in the amygdala. Diffuse VC1.1-ir was also observed in the neuropil of all amygdalar nuclei. Most VC1.1+ PNNs in the rostral third of the amygdala were located in the anterior subdivision of the basolateral nucleus (BLa) and in layers II and III of the nucleus of the lateral olfactory tract (NLOT) (Figs. 1, 2A and 2B). In the middle third of the amygdala most PNNs were seen in the BLa, the posterior subdivision of the basolateral nucleus (BLp), lateral nucleus, and posterolateral cortical nucleus (PLCo) (Figs. 2C, D). In more caudal portions of the amygdala many PNNs were located in the anterolateral amygdalohippocampal area (AHA), as well as in the basal and lateral nuclei (Figs. 2 E, F).

At low and medium powers of magnification it appeared that VC1.1+ PNNs formed a continuous sheath surrounding cell bodies when seen in sections that were perpendicular to their plasma membranes, but observations at higher power revealed that PNNs actually consisted of punctate structures that were either closely apposed to each other or separated by gaps of 0.5 to 2.0 μm (Figs. 3C, D). When viewed en face (in sections that were tangential to plasma membranes) PNNs appeared as true nets with circular or oval openings that were 0.5 to 2.0 μm in diameter (Figs. 3C, 4A). In some cases PNNs extended beyond primary dendrites to also ensheath secondary dendrites (Figs. 3A, D). VC1.1-ir along these dendrites always had a punctate appearance. In the lateral subdivision of the central nucleus no PNNs were observed, but VC1.1-ir was found in irregular clumps in neuronal cell bodies (Fig. 4B).

Although the PNNs were the most conspicuous VC1.1+ structures in the amygdala, there appeared to be a much greater overall quantity of VC1.1-ir in the neuropil of most

amygdalar nuclei. Neuropilar VC1.1-ir was in the form of puncta, or ring-like structures that were 0.5 to 2.0 μm in diameter (Figs. 1, 3). At rostral levels of the amygdala the dorsolateral subdivision of the lateral nucleus (Ld) and anterior basomedial nucleus (BMA) had very dense neuropilar VC1.1-ir, and the BLa had fairly low levels (Fig. 5). At middle levels of the amygdala most nuclei had moderate levels of neuropilar VC1.1-ir, but high levels were seen in dorsolateral lateral nucleus (Ld) and low levels were seen in the BLa (Fig. 6). At levels of the amygdala caudal to the lateral nucleus neuropilar VC1.1-ir was light in the BLp and amygdalohippocampal area, and moderate in the posteromedial cortical nucleus. VC1.1-ir was also seen in the stria terminalis (st), one of the main fiber bundles connecting the amygdala with the hypothalamus and other brain areas (Fig. 6).

Dual-labeling immunohistochemistry using VC1.1 and calcium-binding protein antibodies

The low density of neurons ensheathed by VC1.1+ PNNs in amygdalar nuclei that contained them (basolateral complex, amygdalohippocampal area, cortical nuclei, and NLOT) suggested that they might belong to a subpopulation of nonpyramidal neurons. This was also suggested by the nonpyramidal morphology of some of the cell bodies of these neurons (e.g., the large multipolar cell body of the neuron shown in the upper part of Figure 1B). Since PNNs typically surround PV+ neurons in many CNS areas, we performed dual-labeling for PV and VC1.1 to determine if this was the case for the rat amygdala. This analysis revealed that most neurons ensheathed by VC1.1+ PNNs were PV+ (Figs. 7, 8). Cell counts in the BLa demonstrated that over 90% of neurons ensheathed by VC1.1+ PNNs were PV+, and these VC1.1+/PV+ neurons constituted about 60% of all PV+ neurons (Table 1; Fig. 10). Likewise, it appeared that in other areas of the amygdala with high concentration of VC1.1+ PNNs, the majority of PV+ neurons were VC1.1+ (Figs. 7B, 8). Since the majority of PV+ neurons in the basolateral amygdala also express calbindin (McDonald and Betette, 2001) we analyzed the extent to which VC1.1+ PNNs were associated with CB+ neurons (Fig. 9). Like PV+ neurons, CB+ neurons ensheathed by VC1.1+ PNNs were found in all amygdalar nuclei that exhibited PNNs. Cell counts in the BLa demonstrated that about 70% of neurons ensheathed by VC1.1+ PNNs were CB+, and these VC1.1+/CB+ neurons constituted about 41% of all CB+ neurons (Table 2; Fig. 10).

In the BLa it appeared that PV+ cell bodies that were ensheathed by VC1.1+ PNNs were generally larger than those that were not ensheathed by PNNs. To determine if there were morphological differences in these two types of neurons, the lengths and widths of PV+ cell bodies ensheathed (PV+/VC1.1+ neurons; n = 48) or not ensheathed by PNNs (PV+/VC1.1-negative neurons; n = 37) were measured. The sum of the length and width of each cell body was used as a measure of cell body size, and the ratio of the length and width was used as an indicator of elongation. These measurements revealed that there was a very significant difference in the size of PV+/VC1.1+ cell bodies (M = 28.04 μm, SD = 5.21) compared to PV+/VC1.1-negative cell bodies (M = 24.84 μm, SD = 3.35) ($p < 0.01$), but no significant difference in the elongation of PV+/VC1.1+ cell bodies (M = 1.38, SD = 0.31) compared to PV+/VC1.1-negative cell bodies (M = 1.29, SD = 0.26) ($p > 0.05$). These results indicate that the subpopulation of PV+ neurons in the BLa whose cell bodies are ensheathed by VC1.1+ PNNs are significantly larger than those that are not ensheathed by PNNs, but another morphological feature, elongation, is not different. In fact, all of the cell bodies of PV+

neurons in our quantitative sample whose summed lengths and widths totaled 33 μm or more were ensheathed by VC1.1+ PNNs (Fig. 11).

Colocalization of VC1.1-ir and VVA binding in amygdalar PNNs

The structure of VVA+ PNNs was very similar to that of VC1.1 PNNs (Fig. 12). The distribution of VVA+ PNNs in the amygdala was very similar to that of VC1.1+ PNNS, but they were found in greater numbers (compare Figs. 2 and 13). Cell counts performed using the mirror technique in the BLa revealed that about half (48/94) of all cell bodies that were VC1.1+ or VVA+ were positive for both markers. About 77% of VC1.1+ cell bodies were VVA+, and 60% of VVA+ cell bodies were VC1.1+ (Table 3).

DISCUSSION

This investigation utilized the VC1.1 monoclonal antibody and VVA staining to provide the first detailed maps of PNNs in the rat amygdala. Since the VC1.1 antibody was generated in mice using a homogenate of cat cortical area 17 (Arimatsu et al., 1987) it is not surprising that in the rat amygdala VC1.1+ PNNs were only seen in amygdalar nuclei that have cortex-like cell types (i.e., basolateral nuclei, cortical nuclei, NLOT, and the AHA) (McDonald, 1992), but not in the remaining nuclei (e.g., central and medial nuclei). As in the cortex, VC1.1+ PNNs ensheathed PV+ interneurons in these nuclei. Many of these neurons in the amygdala also expressed calbindin. About half of all PNNs that were VC1.1+ or VVA+ were positive for both markers. However, many VVA+ PNNs were VC1.1-negative. Significant neuropilar VC1.1-ir was seen throughout the amygdala but its density varied in different nuclei.

Morphology, neurochemistry, and distribution of amygdalar VC1.1+ PNNs

The morphology of VC1.1+ PNNs in the amygdala is identical to that of VC1.1+ PNNs in the cortex (Arimatsu et al., 1987; Kosaka et al., 1989). Recent studies indicate that amygdalar PNNs in the rat are immunoreactive for several lecticans, including aggrecan and brevican, as well as tenascin-R (Dauth et al., 2016). Since the VC1.1 antibody recognizes a VC1.1/HNK-1 epitope that is carried by aggrecan and tenascin-R (see Antibody Specificity in Experimental Procedures), many of the PNNs detected by Dauth and co-workers are probably also VC1.1+. In fact, the structure of PNNs in all regions of the CNS are altered in tenascin-R knock-out mice (Brückner et al., 1999).

Electron microscopic studies in the cortex have demonstrated that VC1.1-ir in PNNs is found around axon terminals forming symmetrical (excitatory) or asymmetrical (inhibitory or neuromodulatory) synapses with cell bodies of ensheathed neurons, but not in the presynaptic axon terminals or their synaptic clefts (Naegele et al., 1988). VC1.1-ir was also seen along the cytoplasmic side of the plasma membrane of ensheathed cortical neurons. The morphological similarities in cortical and amygdalar VC1.1+ PNNs suggest that they are associated with the same structures in the amygdala. This is consistent with the size of the fenestrations of the PNNs in the rat amygdala in the present study which are the same size as most axon terminals (0.5 to 2.0 μm in diameter). VC1.1-ir was also seen ensheathing some axon terminals and dendrites in the neuropil of the cortex. This is probably also the

case for the amygdala since VC1.1+ ring-like structures 0.5 to 2.0 μm in diameter (i.e., the size of most axon terminals and dendrites) were seen in the amygdalar neuropil.

VC1.1+ PNNs ensheath subpopulations of calcium-binding expressing interneurons in the rat basolateral amygdala

The present study demonstrated that virtually all of the neurons in the rat amygdala that were ensheathed by VC1.1+ PNNs were PV+. This PV+/VC1.1+ subpopulation constituted about 60% of all PV+ neurons in the BLa. These data are very similar to the results in rat parietal cortex where essentially all VC1.1+ neurons were PV+, and these neurons constitute 66% of all PV+ neurons (Kosaka et al., 1989). Likewise, it appeared that in other areas of the amygdala with high concentrations of VC1.1+ PNNs, the majority of PV+ neurons were ensheathed by PNNs. PV+ neurons constitute about 40% and 20% of GABAergic interneurons, respectively, in the rat basolateral and lateral nuclei, and they are distinct from subpopulations expressing somatostatin, CCK, calretinin, and VIP (McDonald and Mascagni, 2001, 2002; Mascagni and McDonald, 2003). Since it has been estimated that PV + interneurons in BLa constitute about 6% of the entire neuronal population in this nucleus (Mascagni and McDonald, 2003), and 60% are ensheathed by VC1.1+ PNNs, then PV+/ VC1.1+ interneurons appear to make up about 3.6% of the total neuronal population in BLa.

There are actually several subpopulations of PV+ interneurons in the rodent basolateral amygdala that differ in size, electrophysiological characteristics, connectivity, and co-expression of CB (Kemppainen and Pitkänen, 2000; McDonald and Betette, 2001; Rainnie et al., 2006; Woodruff and Sah, 2007; Bienvenu et al., 2012; Vereczki et al., 2016; Veres et al., 2017). On the basis of cell body size (sum of lengths and widths), elongation, and dendritic morphology, Kemppaninen and Pitkänen (2000) described three morphological types of PV+ neurons in the rat basolateral amygdala: (1) Type 1 neurons with small cell bodies; (2) Type 2 neurons with medium-to-large-sized cell bodies; and (3) Type 3 neurons with elongated fusiform cell bodies. Many of the PV+/VC1.1+ neurons in the present study, especially those in the BLa, were among the largest PV+ neurons and thus mainly correspond to Type 2 neurons. Likewise, VC1.1+ PNNs ensheathed GABAergic neurons in the rat visual cortex that had medium to large cell bodies (Naegele et al., 1988). Previous studies have provided evidence that specific electrophysiologically-defined subpopulations of amygdalar PV+ neurons correlate with specific anatomically-defined subpopulations that innervate distinct pyramidal cell domains, including cell bodies (PV+ basket cells), axon initial segments (PV+ chandelier [axo-axonic] cells), or distal dendrites (PV+ dendrite-targeting cells), but the relative size of these subsets of PV+ neurons was not reported (Woodruff and Sah, 2007; Bienvenu et al., 2012). However, Golgi studies (McDonald and Culberson, 1981; McDonald, 1982) have found that chandelier cells, which are now known to be PV+ (McDonald and Betette, 2001; Bienvenu et al., 2012), have relatively large cell bodies. Thus, it seems likely that some of the large PV+/VC1.1+ neurons seen in the present study are chandelier cells (Fig. 11).

In the BLa about 40% of CB+ neurons exhibited VC1.1+ PNNs, and similar percentages of CB+/VC1.1+ neurons were seen in other nuclei of the basolateral amygdala. Approximately 60% of CB+ neurons in the rat BLa were PV+, and PV+/CB+ neurons constituted about

80% of all PV+ neurons (McDonald and Betette, 2001). The finding that 93% of amygdalar VC1.1+ PNNs ensheath PV+ neurons and 70% ensheath CB+ neurons indicates that at least two-thirds of the ensheathed PV+ neurons also express CB. It is of interest in this regard that all PV+ basket cells in the rat basolateral amygdala appear to express CB, but that PV+ chandelier cells do not (Bienvenu et al., 2012; Vereczki et al., 2016). These data are consistent with previous studies which found that pericellular basket-like arrays of immunoreactive axon terminals surrounding pyramidal cell somata are prominent in both CB-stained and PV-stained preparations of the rat basolateral amygdala, and that PV+ axonal cartridges enveloping pyramidal cell axon initial segments are only seen in PV-stained preparations (McDonald, 1997; Kemppainen and Pitkänen, 2000; McDonald and Betette 2001). Collectively, these data, and the cell body size data mentioned previously, suggest that PV+ interneurons ensheathed by VC1.1 PNNs in the basolateral amygdala may include basket cells and chandelier cells.

Colocalization of VC1.1-ir and VVA binding in amygdalar PNNs

Studies in the cortex using the same mirror technique used in the present study demonstrated that about 90% of VC1.1+ neurons were VVA+, and these VC1.1+ neurons constituted about 75% of all VVA+ neurons (Kosaka et al., 1989). Similarly, we found that VVA+ neurons were only located in amygdalar regions that contained VC1.1+ neurons, and about 77% of VC1.1+ neurons in the BLa were also VVA+, constituting 60% of all VVA+ neurons. It is likely that many of the single-labeled VVA+/VC1.1-negative PNNs in the basolateral amygdala ensheath pyramidal cells since WFA, another marker for N-acetylgalactosamines, has been shown to stain PNNs that ensheath these excitatory neurons in this region (Baker et al., 2017; Morikawa et al., 2017). The finding that 93% of VC1.1+ PNNs in the BLa ensheathed PV+ interneurons, suggests that VC1.1+ neurons in the amygdala are largely a subset of VVA+ GABAergic interneurons. As discussed above, many of these amygdalar PV+/VC1.1 interneurons may be basket or chandelier cells. In the visual cortex, however, large basket cells, but not chandelier cells exhibit WFA+ PNNs (Naegele and Katz, 1990). In the hippocampus 90% of WFA+ PNNs ensheath basket cells, but very few ensheath chandelier cells (Yamada and Jinno, 2015). Future studies combining analysis of axonal morphology of individual neurons with VC1.1 immunohistochemistry will be necessary to definitely determine which PV subpopulations in the basolateral amygdala are ensheathed by VC1.1+ PNNs.

Functional Significance

The electrophysiological significance of PNNs surrounding PV+ interneurons has not been studied in the amygdala, but has been investigated in the neocortex. Most PNNs in the rat and monkey neocortex ensheath fast-firing PV+ interneurons that express potassium channel Kv3.1b subunits, which are critical for producing the short-duration action potentials required for high-frequency firing (Härtig et al., 1999). These findings suggested that PNNs might be necessary for this fast-spiking phenotype. However, the results of a recent study of fast-spiking GABAergic PV+ neurons of the neocortex, as well as fast-spiking glycinergic neurons of the medial trapezoid nucleus of the brainstem, suggests that this is not the case. In recordings from brain slices in which PNNs were degraded by chondroitinase (by breaking down GAGs of chondroitin sulfate proteoglycans), it was found that there was no

change in passive membrane properties in these neurons, or in their ability to fire rapid short-duration action potentials, but that there was reduced and delayed spiking (Balmer 2016). Similar results were obtained in brevican knock-out mice (Blosa et al., 2015). Thus, it appears that PNNs increase the excitability of the ensheathed neurons in response to synaptic inputs.

Electrophysiological studies have demonstrated that subpopulations of PV+ neurons in the basolateral amygdala, like those in the cortex, exhibit high-frequency firing (Rainnie et al., 2006; Woodruff and Sah, 2007) and are the main interneuronal subtype expressing Kv3.1b subunits (McDonald and Mascagni, 2006). Consistent with the finding that PNNs are not required for the fast-firing phenotype (Balmer 2016), 96% of PV+ neurons in the BLa expressed Kv3.1b (McDonald and Mascagni, 2006), but only 60% were ensheathed by VC1.1+ PNNs (present study). In addition, many WFA+ PNNs in the cortex and basolateral amygdala ensheath pyramidal cells (Wegner et al., 2003; Alpár et al., 2006; Morikawa et al., 2017), and it is well established that pyramidal cells in the basolateral amygdala, like those in the cortex, are not fast-spiking (McDonald et al., 2005; Pape et al., 2005). Thus, it seems likely that one of the main roles of PNNs in the basolateral amygdala, like those in the neocortex, may be to increase the excitability of the PV+ neurons rather than being essential for fast-spiking. It has been suggested that PNNs, which are negatively charged (Brückner et al., 1993), may do this by several possible mechanisms including: (1) shifting the activation of voltage-dependent ionic currents to lower voltages; (2) maintaining a perineuronal buffering system for Na^+ and K^+ ions; and/or (3) promoting clustering of AMPA receptors and Na^+ and K^+ channels (Balmer, 2016).

There is extensive evidence that PNNs regulate synaptic plasticity (for reviews see Dityatev and Schachner, 2003; Hensch, 2005; Galtrey and Fawcett, 2007; Wang and Fawcett 2012; Sorg et al., 2016). PNNs form postnatally in an activity-dependent manner, and have been shown to mark the end of “critical periods” in the development of several systems including the ocular dominance columns of the visual cortex and the barrels of the somatosensory cortex (Wang and Fawcett, 2012). Synaptic plasticity during critical periods involves synaptogenesis and the formation of the basic circuits of these sensory systems. PNNs appear to stabilize these basic synaptic connections and tend to restrict further synaptic plasticity. It has been suggested that PNNs may restrict synaptic plasticity by: (1) forming a physical barrier between neurons and incoming axons; (2) providing a scaffold which binds molecules that inhibit the formation of new synapses; and/or (3) restricting the lateral mobility of AMPA receptors (Wang and Fawcett 2012; Sorg et al., 2016).

PNNs have also been shown to regulate synaptic plasticity involved in memory formation and erasure in the rat amygdala. The formation of PNNs in the basolateral amygdala during postnatal days 16-21 protect fear memories from erasure during extinction training (Gogolla et al., 2009). Fear conditioning memories formed before this critical postnatal period can be erased by extinction training whereas those formed after PNNs are formed cannot be erased. Injections of chondroitinase to deplete PNNs in the basolateral amygdala restored the juvenile condition in which extinguished fear memories cannot be restored by spontaneous recovery or context-dependent renewal training (Gogolla et al., 2009). Likewise, it has been found that intra-amygdalar injections of chondroitinase combined with extinction training

erased drug-induced conditioned place preference memory in rats (Xue et al., 2014). Although it is known that amygdalar PV+ interneurons are critical for inhibitory and disinhibitory influences during conditioning and extinction (Trouche et al., 2013; Wolff et al., 2014), the exact mechanism by which PNNs surrounding these interneurons prevent the erasure of memories has yet to be determined. Since one function of PNNs is the stabilization of synapses, it would appear that long-term potentiation of synapses or other forms of synaptic plasticity involved in conditioning may be protected from further alterations, such as depotentiation, by the presence of PNNs. It remains to be determined how PNNs are critical for this change and whether chondroitin sulphate proteoglycans in the neuropil (diffuse extracellular matrix), which are also degraded by chondroitinase, play a role. It has been proposed that long-term memories are stored in the pattern of holes in PNNs occupied by axon terminals (Tsien, 2013).

Gogolla and co-workers (2009) found that chondroitinase injections into the basolateral amygdala completely abolished LTP of monosynaptic excitatory thalamic inputs to lateral nucleus pyramidal cells and significantly reduced LTP of disynaptic inhibition of pyramidal cells in amygdalar slices. It is possible that reduced LTP of disynaptic inhibition, which entails glutamatergic inputs to feedforward interneurons, could involve excitatory thalamic inputs onto PV+ interneurons which have had their PNNs degraded since PV+ interneurons in the lateral nucleus receive potent excitatory inputs from the thalamus and mediate feedforward inhibition onto pyramidal cells (Woodson et al., 2000; Lucas et al., 2016). A decrease in the excitability of these PV+ interneurons, which occurs in cortical PV+ neurons with degraded PNNs (see above), might contribute to the reduction in LTP. It is not clear if the complete elimination of LTP of monosynaptic excitatory thalamic inputs to lateral nucleus pyramidal cells is related to breakdown of PNNs around PV+ interneurons or is related to the breakdown of the diffuse neuropilar extracellular matrix.

CONCLUSIONS

This study demonstrates that monoclonal antibody VC1.1, whose epitope has been shown in previous studies to be the same carbohydrate moiety recognized by the HNK-1 monoclonal antibody, stains PNNs ensheathing a subpopulation of PV+ interneurons in the cortex-like amygdalar nuclei of the rat, including the basolateral nuclear complex. These amygdalar VC1.1 PNNs are largely a subset of VVA+ PNNs that express N-acetylgalactosamine. Most PV+/VC1.1+ interneurons also express CB, and many may correspond to a subpopulation of large PV+ interneurons known to provide a perisomatic innervation of pyramidal cells. Although less conspicuous, there is also significant neuropilar VC1.1-ir whose density varied in different amygdalar nuclei. Since electrophysiological studies suggest that the VC1.1/HNK-1 glycan modulates LTP in the hippocampus (Saghatelyan et al., 2000, 2001; Bukalo et al., 2001), it may also play a similar role in the alterations of LTP and the encoding of fear and drug-related memories associated with PNNs in the basolateral amygdala. There is a loss of PNNs surrounding GABAergic interneurons in the basolateral amygdala in schizophrenia (Pantazopoulos et al., 2010, 2015; Berretta et al., 2015; Pantazopoulos and Berretta 2016), which may be associated with altered fear learning seen in this disorder (Holt et al., 2009). The finding that PNNs and other components of the extracellular matrix are altered in neuropsychiatric diseases suggests that a greater

understanding of their structure and function could lead to novel therapies to treat these disorders.

Acknowledgments

The authors thank Dr. Kenneth G. Baimbridge (University of British Columbia) for his generous donation of the PV and CB polyclonal antisera. This work was supported by NIH Grants R01MH104638 and R01NS19733.

References

Abo T, Balch CM. A differentiation antigen of human NK and K cells identified by a monoclonal antibody (HNK-1). J Immunol. 1981; 127:1024–1029. [PubMed: 6790607]

Alpár A, Gärtner U, Härtig W, Brückner G. Distribution of pyramidal cells associated with perineuronal nets in the neocortex of rat. Brain Res. 2006; 1120:13–22. [PubMed: 16996045]

Arimatsu Y, Naegele JR, Barnstable CJ. Molecular markers of neuronal subpopulations in layers 4, 5, and 6 of cat primary visual cortex. J Neurosci. 1987; 7:1250–1263. [PubMed: 3553447]

Baker KD, Gray AR, Richardson R. The development of perineuronal nets around parvalbumin gabaergic neurons in the medial prefrontal cortex and basolateral amygdala of rats. Behav Neurosci. 2017; 131:289–303. [PubMed: 28714715]

Balmer TS. Perineuronal Nets Enhance the Excitability of Fast-Spiking Neurons. eNeuro. 2016 Jul 27.3(4)

Barnstable CJ, Kosaka T, Naegele JR, Arimatsu Y. Molecular properties of GABAergic local-circuit neurons in the mammalian visual cortex. Prog Brain Res. 1992; 90:503–522. [PubMed: 1631310]

Bekku Y, Rauch U, Ninomiya Y, Oohashi T. Brevican distinctively assembles extracellular components at the large diameter nodes of Ranvier in the CNS. J Neurochem. 2009; 108:1266–1276. [PubMed: 19141078]

Berretta S. Extracellular matrix abnormalities in schizophrenia. Neuropharmacology. 2012; 62:1584–1597. [PubMed: 21856318]

Berretta S, Pantazopoulos H, Markota M, Brown C, Batzianouli ET. Losing the sugar coating: potential impact of perineuronal net abnormalities on interneurons in schizophrenia. Schizophr Res. 2015; 167:18–27. [PubMed: 25601362]

Bienvenu TC, Busti D, Magill PJ, Ferraguti F, Capogna M. Cell-type-specific recruitment of amygdala interneurons to hippocampal theta rhythm and noxious stimuli in vivo. Neuron. 2012; 74:1059–1074. [PubMed: 22726836]

Blosa M, Sonntag M, Jäger C, Weigel S, Seeger J, Frischknecht R, Seidenbecher CI, Matthews RT, Arendt T, Rübsamen R, Morawski M. The extracellular matrix molecule brevican is an integral component of the machinery mediating fast synaptic transmission at the calyx of Held. J Physiol. 2015; 593:4341–4360. [PubMed: 26223835]

Brückner G, Brauer K, Härtig W, Wolff JR, Rickmann MJ, Derouiche A, Delpech B, Girard N, Oertel WH, Reichenbach A. Perineuronal nets provide a polyanionic, glia-associated form of microenvironment around certain neurons in many parts of the rat brain. Glia. 1993; 8:183–200. [PubMed: 7693589]

Brückner G, Grosche J, Schmidt S, Härtig W, Margolis RU, Delpech B, Seidenbecher CI, Czaniera R, Schachner M. Postnatal development of perineuronal nets in wild-type mice and in a mutant deficient in tenascin-R. J Comp Neurol. 1999; 428:616–629.

Bukalo O, Schachner M, Dityatev A. Modification of extracellular matrix by enzymatic removal of chondroitin sulfate and by lack of tenascin-R differentially affects several forms of synaptic plasticity in the hippocampus. Neuroscience. 2001; 104:359–369. [PubMed: 11377840]

Carulli D, Rhodes KE, Brown DJ, Bonnert TP, Pollack SJ, Oliver K, Strata P, Fawcett JW. Composition of perineuronal nets in the adult rat cerebellum and the cellular origin of their components. J Comp Neurol. 2006; 494:559–577. [PubMed: 16374793]

Celio MR, Blümcke I. Perineuronal nets–a specialized form of extracellular matrix in the adult nervous system. Brain Res Brain Res Rev. 1994; 19:128–145. [PubMed: 8167657]

Celio MR, Spreafico R, De Biasi S, Vitellaro-Zuccarello L. Perineuronal nets: past and present. Trends Neurosci. 1998; 21:510–515. [PubMed: 9881847]

Condé F, Lund JS, Jacobowitz DM, Baimbridge KG, Lewis DA. Local circuit neurons immunoreactive for calretinin, calbindin D-28k or parvalbumin in monkey prefrontal cortex: distribution and morphology. J Comp Neurol. 1994; 341:95–116. [PubMed: 8006226]

Dauth S, Grevesse T, Pantazopoulos H, Campbell PH, Maoz BM, Berretta S, Parker KK. Extracellular matrix protein expression is brain region dependent. J Comp Neurol. 2016; 524:1309–1336. [PubMed: 26780384]

Dityatev A, Schachner M. Extracellular matrix molecules and synaptic plasticity. Nat Rev Neurosci. 2003; 4:456–468. [PubMed: 12778118]

Galtrey CM, Fawcett JW. The role of chondroitin sulfate proteoglycans in regeneration and plasticity in the central nervous system. Brain Res Rev. 2007; 54:1–18. [PubMed: 17222456]

Gogolla N, Caroni P, Lüthi A, Herry C. Perineuronal nets protect fear memories from erasure. Science. 2009; 325:1258–1261. [PubMed: 19729657]

Golgi C. Intorno all'origine del quarto nervo cerebrale e una questione isto-fisiologica che a questo argomento si collega. Rendiconti della Reale Accademia dei Lincei (21 maggio). 1893; 2:443–450.

Hancock MB. Two-color immunoperoxidase staining: visualization of anatomic relationships between immunoreactive neural elements. Am J Anat. 1986; 175:343–352. [PubMed: 2422916]

Härtig W, Brückner G, Brauer K, Schmidt C, Bigl V. Allocation of perineuronal nets and parvalbumin-, calbindin-D28k- and glutamic acid decarboxylase-immunoreactivity in the amygdala of the rhesus monkey. Brain Res. 1995; 698:265–269. [PubMed: 8581495]

Härtig W, Derouiche A, Welt K, Brauer K, Grosche J, Mäder M, Reichenbach A, Brückner G. Cortical neurons immunoreactive for the potassium channel Kv3.1b subunit are predominantly surrounded by perineuronal nets presumed as a buffering system for cations. Brain Res. 1999; 842:15–29. [PubMed: 10526091]

Hensch TK. Critical period plasticity in local cortical circuits. Nat Rev Neurosci. 2005; 6:877–888. [PubMed: 16261181]

Holt DJ, Lebron-Milad K, Milad MR, Rauch SL, Pitman RK, Orr SP, Cassidy BS, Walsh JP, Goff DC. Extinction memory is impaired in schizophrenia. Biol Psychiatry. 2009; 65:455–463. [PubMed: 18986648]

Horii-Hayashi N, Sasagawa T, Matsunaga W, Nishi M. Development and structural variety of the chondroitin sulfate proteoglycans-contained extracellular matrix in the mouse brain. Neural Plast. 2015; 2015:256389. [PubMed: 26649203]

Kemppainen S, Pitkänen A. Distribution of parvalbumin, calretinin, and calbindin-D(28k) immunoreactivity in the rat amygdaloid complex and colocalization with gamma-aminobutyric acid. J Comp Neurol. 2000; 426:441–467. [PubMed: 10992249]

Kizuka Y, Oka S. Regulated expression and neural functions of human natural killer-1 (HNK-1) carbohydrate. Cell Mol Life Sci. 2012; 69:4135–4147. [PubMed: 22669261]

Kosaka T, Heizmann CW, Barnstable CJ. Monoclonal antibody VC1.1 selectively stains a population of GABAergic neurons containing the calcium-binding protein parvalbumin in the rat cerebral cortex. Exp Brain Res. 1989; 78:43–50. [PubMed: 2591517]

Kosaka T, Isogai K, Barnstable CJ, Heizmann CW. Monoclonal antibody HNK-1 selectively stains a subpopulation of GABAergic neurons containing the calcium-binding protein parvalbumin in the rat cerebral cortex. Exp Brain Res. 1990; 82:566–574. [PubMed: 1705516]

Lucas EK, Jegarl AM, Morishita H, Clem RL. Multimodal and site-specific plasticity of amygdala parvalbumin interneurons after fear learning. Neuron. 2016; 91:629–643. [PubMed: 27427462]

Maeda N. Proteoglycans and neuronal migration in the cerebral cortex during development and disease. Front Neurosci. 2015; 9:98. [PubMed: 25852466]

Mascagni F, McDonald AJ. Immunohistochemical characterization of cholecystokinin containing neurons in the rat basolateral amygdala. Brain Res. 2003; 976:171–184. [PubMed: 12763251]

Mascagni F, Muly EC, Rainnie DG, McDonald AJ. Immunohistochemical characterization of parvalbumin-containing interneurons in the monkey basolateral amygdala. Neuroscience. 2009; 158:1541–1550. [PubMed: 19059310]

Matthews RT, Kelly GM, Zerillo CA, Gray G, Tiemeyer M, Hockfield S. Aggrecan glycoforms contribute to the molecular heterogeneity of perineuronal nets. J Neurosci. 2002; 22:7536–7547. [PubMed: 12196577]

McDonald AJ, Culberson JL. Neurons of the basolateral amygdala: a Golgi study in the opossum (Didelphis virginiana). Am J Anat. 1981; 162:327–342. [PubMed: 7325125]

McDonald AJ. Neurons of the lateral and basolateral amygdaloid nuclei: a Golgi study in the rat. J Comp Neurol. 1982; 212:293–312. [PubMed: 6185547]

McDonald, AJ. Cell types and intrinsic connections of the amygdala. In: Aggleton, JP., editor. The amygdala. New York: Wiley-Liss; 1992. p. 67-96.

McDonald AJ. Calbindin-D28k immunoreactivity in the rat amygdala. J Comp Neurol. 1997; 383:231–244. [PubMed: 9182851]

McDonald AJ, Betette RL. Parvalbumin-containing neurons in the rat basolateral amygdala: morphology and co-localization of calbindin-D(28k). Neuroscience. 2001; 102:413–425. [PubMed: 11166127]

McDonald AJ, Mascagni F. Colocalization of calcium-binding proteins and GABA in neurons of the rat basolateral amygdala. Neuroscience. 2001; 105:681–693. [PubMed: 11516833]

McDonald AJ, Mascagni F. Immunohistochemical characterization of somatostatin containing interneurons in the rat basolateral amygdala. Brain Res. 2002; 943:237–244. [PubMed: 12101046]

McDonald AJ, Mascagni F, Mania I, Rainnie DG. Evidence for a perisomatic innervation of parvalbumin-containing interneurons by individual pyramidal cells in the basolateral amygdala. Brain Res. 2005; 1035:32–40. [PubMed: 15713274]

McDonald AJ, Mascagni F. Differential expression of Kv3.1b and Kv3.2 potassium channel subunits in interneurons of the basolateral amygdala. Neuroscience. 2006; 138:537–547. [PubMed: 16413129]

Morikawa S, Ikegaya Y, Narita M, Tamura H. Activation of perineuronal net-expressing excitatory neurons during associative memory encoding and retrieval. Sci Rep. 2017; 7:46024. [PubMed: 28378772]

Mueller AL, Davis A, Sovich S, Carlson SS, Robinson FR. Distribution of n-acetylgalactosamine-positive perineuronal nets in the macaque brain: Anatomy and Implications. Neural Plast. 2016; 2016:6021428. [PubMed: 26881119]

Naegele JR, Katz LC. Cell surface molecules containing N-acetylgalactosamine are associated with basket cells and neurogliaform cells in cat visual cortex. J Neurosci. 1990; 10:540–557. [PubMed: 2303859]

Naegele JR, Barnstable CJ. A carbohydrate epitope defined by monoclonal antibody VC1.1 is found on N-CAM and other cell adhesion molecules. Brain Res. 1991; 559:118–129. [PubMed: 1723642]

Pantazopoulos H, Lange N, Hassinger L, Berretta S. Subpopulations of neurons expressing parvalbumin in the human amygdala. J Comp Neurol. 2006; 496:706–722. [PubMed: 16615121]

Pantazopoulos H, Murray EA, Berretta S. Total number, distribution, and phenotype of cells expressing chondroitin sulfate proteoglycans in the normal human amygdala. Brain Res. 2008; 1207:84–95. [PubMed: 18374308]

Pantazopoulos H, Woo TU, Lim MP, Lange N, Berretta S. Extracellular matrix-glial abnormalities in the amygdala and entorhinal cortex of subjects diagnosed with schizophrenia. Arch Gen Psychiatry. 2010; 67:155–166. [PubMed: 20124115]

Pantazopoulos H, Markota M, Jaquet F, Ghosh D, Wallin A, Santos A, Caterson B, Berretta S. Aggrecan and chondroitin-6-sulfate abnormalities in schizophrenia and bipolar disorder: a postmortem study on the amygdala. Transl Psychiatry. 2015; 5:e496. [PubMed: 25603412]

Pantazopoulos H, Berretta S. In Sickness and in Health: Perineuronal Nets and Synaptic Plasticity in Psychiatric Disorders. Neural Plast. 2016; 2016:9847696. [PubMed: 26839720]

Pape HC, Narayanan RT, Smid J, Stork O, Seidenbecher T. Theta activity in neurons and networks of the amygdala related to long-term fear memory. Hippocampus. 2005; 15:874–880. [PubMed: 16158424]

Paxinos, G., Watson, C. The rat brain in stereotaxic coordinates. Academic Press; New York: 1997. 1997

Rainnie DG, Mania I, Mascagni F, McDonald AJ. Physiological and morphological characterization of parvalbumin-containing interneurons of the rat basolateral amygdala. J Comp Neurol. 2006; 498:142–161. [PubMed: 16856165]

Ren JQ, Heizmann CW, Kosaka T. Regional difference in the distribution of parvalbumin-containing neurons immunoreactive for monoclonal antibody HNK-1 in the mouse cerebral cortex. Neurosci Lett. 1994; 166:221–225. [PubMed: 8177503]

Saghatelyan AK, Gorissen S, Albert M, Hertlein B, Schachner M, Dityatev A. The extracellular matrix molecule tenascin-R and its HNK-1 carbohydrate modulate perisomatic inhibition and long-term potentiation in the CA1 region of the hippocampus. Eur J Neurosci. 2000; 12:3331–33342. [PubMed: 10998116]

Saghatelyan AK, Dityatev A, Schmidt S, Schuster T, Bartsch U, Schachner M. Reduced perisomatic inhibition, increased excitatory transmission, and impaired long-term potentiation in mice deficient for the extracellular matrix glycoprotein tenascin-R. Mol Cell Neurosci. 2001; 17:226–240. [PubMed: 11161481]

Smith PD, Coulson-Thomas VJ, Foscarin S, Kwok JC, Fawcett JW. “GAG-ing with the neuron”: The role of glycosaminoglycan patterning in the central nervous system. Exp Neurol. 2015; 274(Pt B): 100–114. [PubMed: 26277685]

Sorg BA, Berretta S, Blacktop JM, Fawcett JW, Kitagawa H, Kwok JC, Miquel M. Casting a Wide Net: Role of Perineuronal Nets in Neural Plasticity. J Neurosci. 2016; 36:11459–11468. [PubMed: 27911749]

Trouche S, Sasaki JM, Tu T, Reijmers LG. Fear extinction causes target-specific remodeling of perisomatic inhibitory synapses. Neuron. 2013; 80:1054–1065. [PubMed: 24183705]

Tsien RY. Very long-term memories may be stored in the pattern of holes in the perineuronal net. Proc Natl Acad Sci U S A. 2013; 110:12456–12461. [PubMed: 23832785]

Umemori J, Winkel F, Castrén E, Karpova NN. Distinct effects of perinatal exposure to fluoxetine or methylmercury on parvalbumin and perineuronal nets, the markers of critical periods in brain development. Int J Dev Neurosci. 2015; 44:55–64. [PubMed: 25997908]

Vereczki VK, Veres JM, Müller K, Nagy GA, Rácz B, Barsy B, Hájos N. Synaptic organization of perisomatic GABAergic inputs onto the principal cells of the mouse basolateral amygdala. Front Neuroanat. 2016; 10:20. [PubMed: 27013983]

Veres JM, Nagy GA, Hájos N. Perisomatic GABAergic synapses of basket cells effectively control principal neuron activity in amygdala networks. Elife. 2017 Jan 6.6:pii, e20721. 2017.

Viapiano MS, Matthews RT. From barriers to bridges: chondroitin sulfate proteoglycans in neuropathology. Trends Mol Med. 2006; 12:488–496. [PubMed: 16962376]

Wang D, Fawcett J. The perineuronal net and the control of CNS plasticity. Cell Tissue Res. 2012; 349:147–160. [PubMed: 22437874]

Weber P, Bartsch U, Rasband MN, Czaniera R, Lang Y, Bluethmann H, Margolis RU, Levinson SR, Shrager P, Montag D, Schachner M. Mice deficient for tenascin-R display alterations of the extracellular matrix and decreased axonal conduction velocities in the CNS. J Neurosci. 1999; 19:4245–4262. [PubMed: 10341229]

Wegner F, Härtig W, Bringmann A, Grosche J, Wohlfarth K, Zuschratter W, Brückner G. Diffuse perineuronal nets and modified pyramidal cells immunoreactive for glutamate and the GABA(A) receptor alpha1 subunit form a unique entity in rat cerebral cortex. Exp Neurol. 2003; 184:705–714. [PubMed: 14769362]

Wolff SB, Gründemann J, Tovote P, Krabbe S, Jacobson GA, Müller C, Herry C, Ehrlich I, Friedrich RW, Letzkus JJ, Lüthi A. Amygdala interneuron subtypes control fear learning through disinhibition. Nature. 2014; 509:453–458. [PubMed: 24814341]

Woodruff AR, Sah P. Networks of parvalbumin-positive interneurons in the basolateral amygdala. J Neurosci. 2007; 27:553–563. [PubMed: 17234587]

Woodson W, Farb CR, Ledoux JE. Afferents from the auditory thalamus synapse on inhibitory interneurons in the lateral nucleus of the amygdala. Synapse. 2000; 38:124–137. [PubMed: 11018786]

Xue YX, Xue LF, Liu JF, He J, Deng JH, Sun SC, Han HB, Luo YX, Xu LZ, Wu P, Lu L. Depletion of perineuronal nets in the amygdala to enhance the erasure of drug memories. J Neurosci. 2014; 34:6647–6658. [PubMed: 24806690]

Yamada J, Jinno S. Subclass-specific formation of perineuronal nets around parvalbumin-expressing GABAergic neurons in Ammon's horn of the mouse hippocampus. J Comp Neurol. 2015; 523:790–804. [PubMed: 25420705]

Yamamoto M, Marshall P, Hemmendinger LM, Boyer AB, Caviness VS Jr. Distribution of glucuronic acid-and-sulfate-containing glycoproteins in the central nervous system of the adult mouse. Neurosci Res. 1988; 5:273–298. [PubMed: 2453818]

Zaremba S, Naegele JR, Barnstable CJ, Hockfield S. Neuronal subsets express multiple high-molecular-weight cell-surface glycoconjugates defined by monoclonal antibodies Cat-301 and VC1.1. J Neurosci. 1990; 10:2985–2995. [PubMed: 2204685]

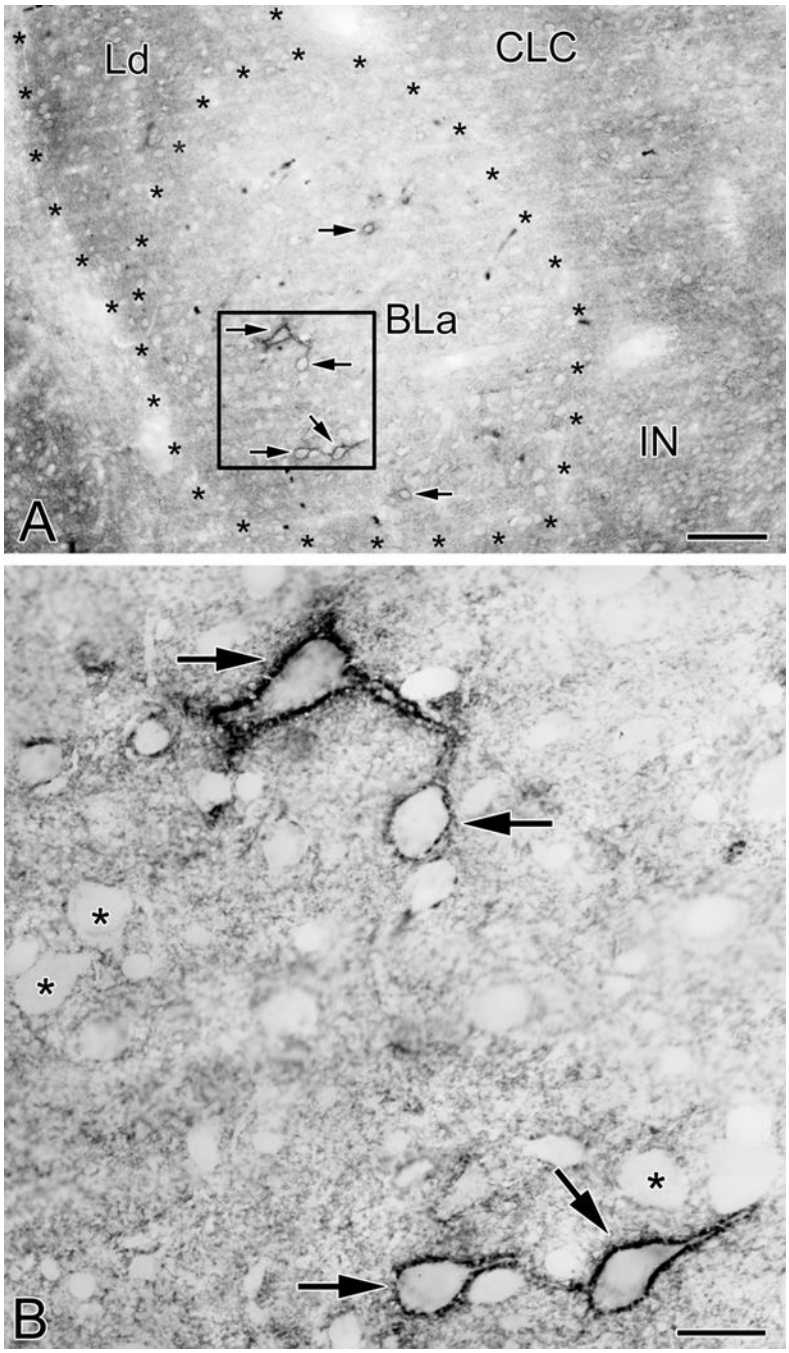

Fig. 1.

VC1.1-ir in PNNs and the neuropil in the anterior subdivision of the basolateral nucleus (BLa). (A) Photomicrograph of VC1.1-ir in the BLa at the bregma −1.8 level. Asterisks indicate the borders of BLa and the dorsolateral subdivision of the lateral nucleus (Ld). Four neurons ensheathed by VC1.1+ PNNs are in the boxed area of BLa (arrows; see B). Two additional BLa neurons ensheathed by VC1.1+ PNNs are also indicated by arrows. Other abbreviations: CLC, lateral capsular subdivision of the central nucleus; IN, intercalated nucleus. (B) Higher power photomicrograph of the boxed area in A. Note punctate VC1.1-ir

in the neuropil and along the plasma membranes of the cell bodies and proximal dendrites of four neurons (arrows). In addition, some VC1.1-ir in the neuropil is in the form of small rings that are 1-2 μm in diameter. Asterisks indicate representative neurons that are not ensheathed by PNNs, but whose plasma membranes are decorated by punctate neuropilar VC1.1-ir. *Scale bars = 100 μm in A, 20 μm in B*

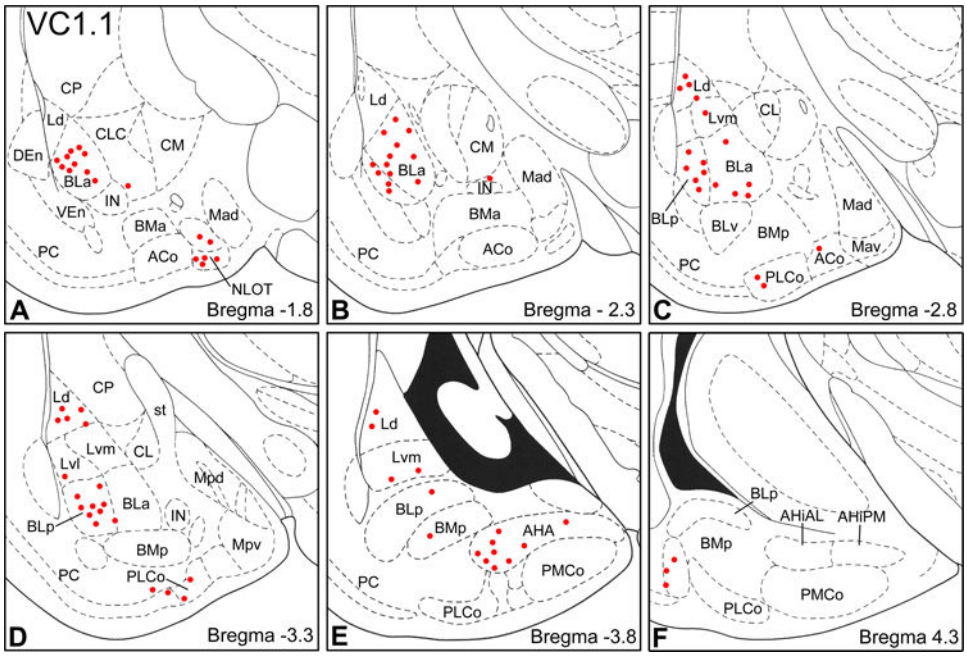

Fig. 2.

Distribution of VC1.1+ PNNs in the amygdala (red dots) in sections arranged from rostral (A) to caudal (F). Each bregma level shows the locations of neurons plotted from three non-adjacent 50 μm-thick sections; each dot represents one neuron. Templates are modified from the atlas by Paxinos and Watson (1997). Abbreviations: ACo, anterior cortical nucleus; AHA, amygdalohippocampal area; AHiAL, anterolateral amygdalohippocampal area; AHiPM, posteromedial amygdalohippocampal area; BLa, anterior basolateral nucleus; BLp, posterior basolateral nucleus; BLv, ventral basolateral nucleus; BMa, anterior basomedial nucleus; BMp, posterior basomedial nucleus; CL, lateral central nucleus; CLC, lateral capsular subdivision of the central nucleus; CM, medial central nucleus; CP, caudate putamen; DEn, dorsal endopiriform nucleus; IN, intercalated nucleus; Ld, dorsolateral lateral nucleus; Lvl, ventrolateral lateral nucleus; Lvm, ventromedial lateral nucleus; Mad, anterodorsal medial nucleus; Mav, anteroventral medial nucleus; Mpd, posterodorsal medial nucleus; Mpv, posteroventral medial nucleus; NLOT, nucleus of the lateral olfactory tract; PC, piriform cortex; PLCo, posterolateral cortical nucleus; PMCo, posteromedial cortical nucleus; st, stria terminalis; VEn, ventral endopiriform nucleus.

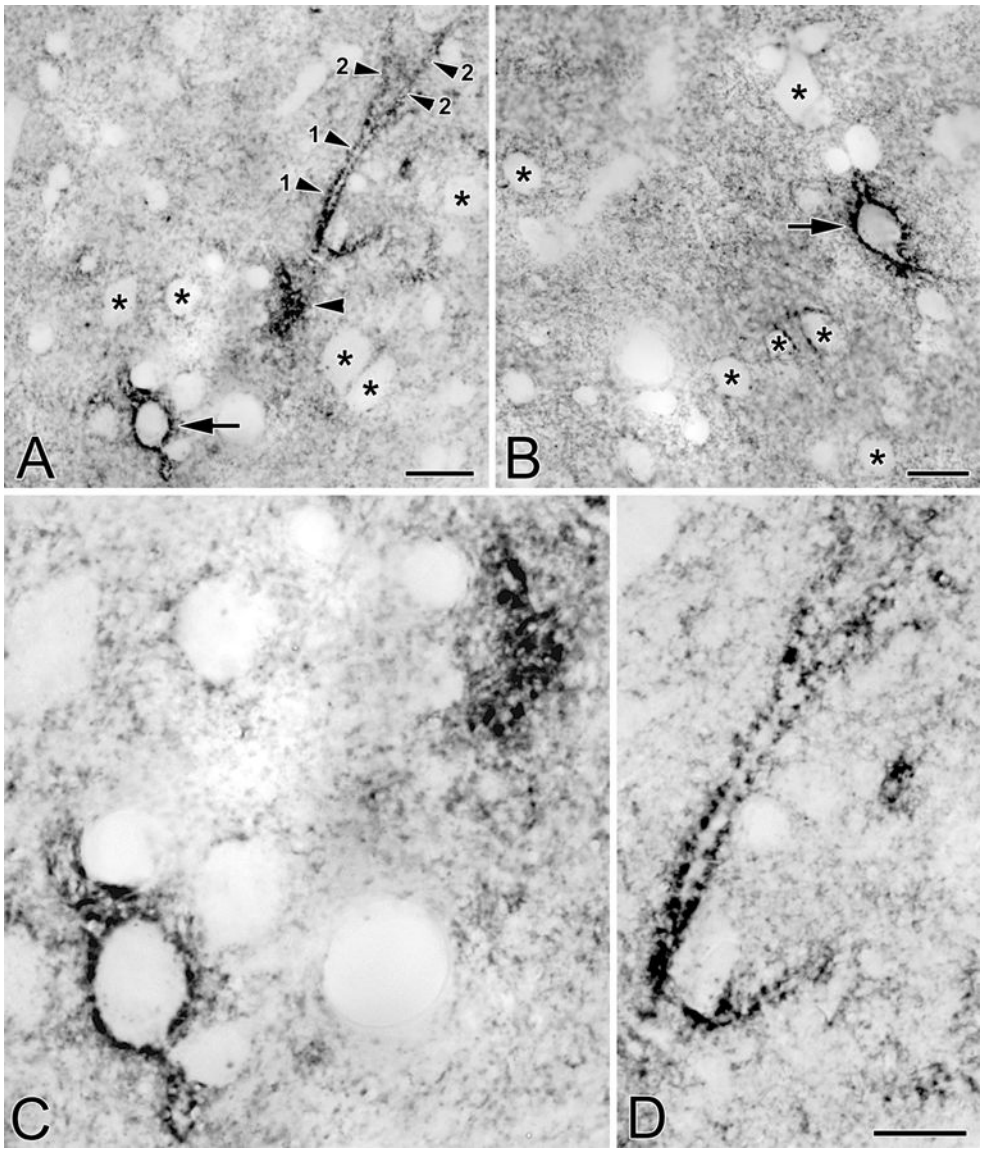

Fig. 3.

(A) Photomicrograph of a neuron in the BLa that is ensheathed by a VC1.1+ PNN (arrow). Also in the field is a primary dendrite (1) and two secondary dendrites (2) of another neuron. Only the edge of the cell body giving rise to these dendrites was in this section (unlabeled arrowhead). (B) Photomicrograph of a neuron in the lateral nucleus that is ensheathed by a VC1.1+ PNN (arrow). (C) Higher power view of the cell bodies in A. (D) Higher power view of the dendrites in A. Asterisks in A, B and C indicate representative neurons that are not ensheathed by PNNs, but whose plasma membranes are decorated by punctate neuropilar VC1.1-ir. *Scale bars = 20 μm for A and B; 10 μm in D (C is at the same magnification)*

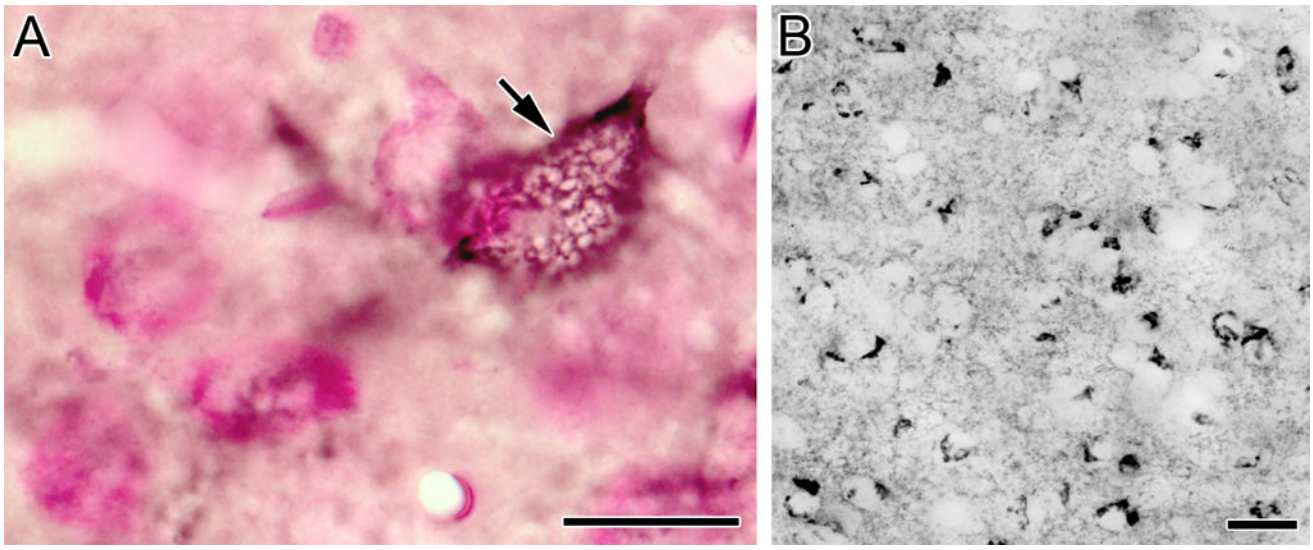

Fig. 4.

(A) Photomicrograph of a VC1.1+ PNN (black) surrounding the cell body of a BLa neuron (arrow) in a pyronin Y counterstained section. This en face view of the VC1.1+ lattice coating the plasma membrane of this cell shows ovoid gaps that probably correspond to locations where axon terminals are forming synaptic contacts with this cell body. (B) VC1.1-ir in the lateral subdivision of the central nucleus. *Scale bars = 20 μm*

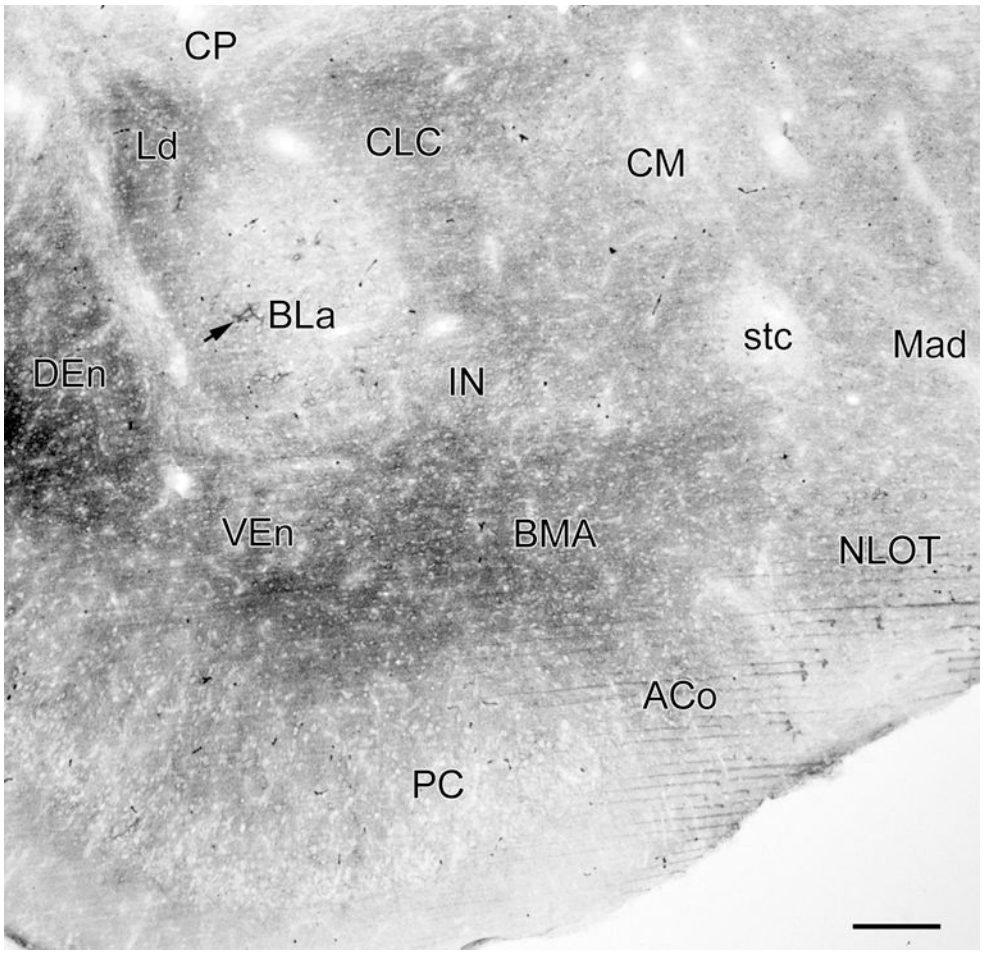

Fig. 5.

Photomicrograph of VC1.1-ir in a coronal section through the rostral amygdala (bregma −1.8 level; compare with Fig. 2A; see caption of Fig. 2 for abbreviations). Figure 1A is a higher power photomicrograph of the BLa in this section. Arrow indicates a large neuron in the anterior subdivision of the basolateral nucleus (BLa) that is ensheathed by a VC1.1+ PNN. There are 5 additional PNNs in the BLa in this section, and 3 in the nucleus of the lateral olfactory tract (NLOT), but they are difficult to see at this low magnification. Thus, almost all of the VC1.1-ir seen in this section is in the neuropil. *Scale bar = 200 μm*

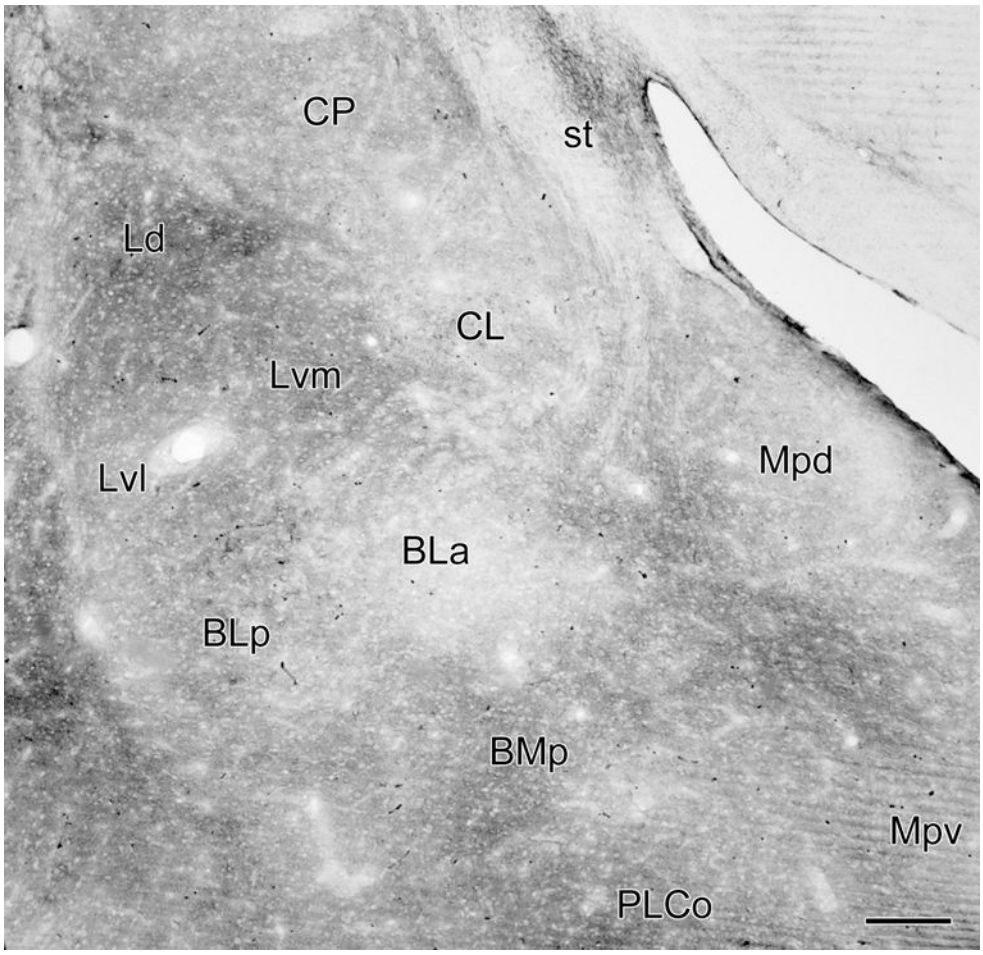

Fig. 6.

Photomicrograph of VC1.1-ir in a coronal section through the middle of the amygdala (bregma −3.3 level; compare with Fig. 2D). Almost all of the VC1.1-ir seen in this section is in the neuropil. *Scale bar = 200 μm*

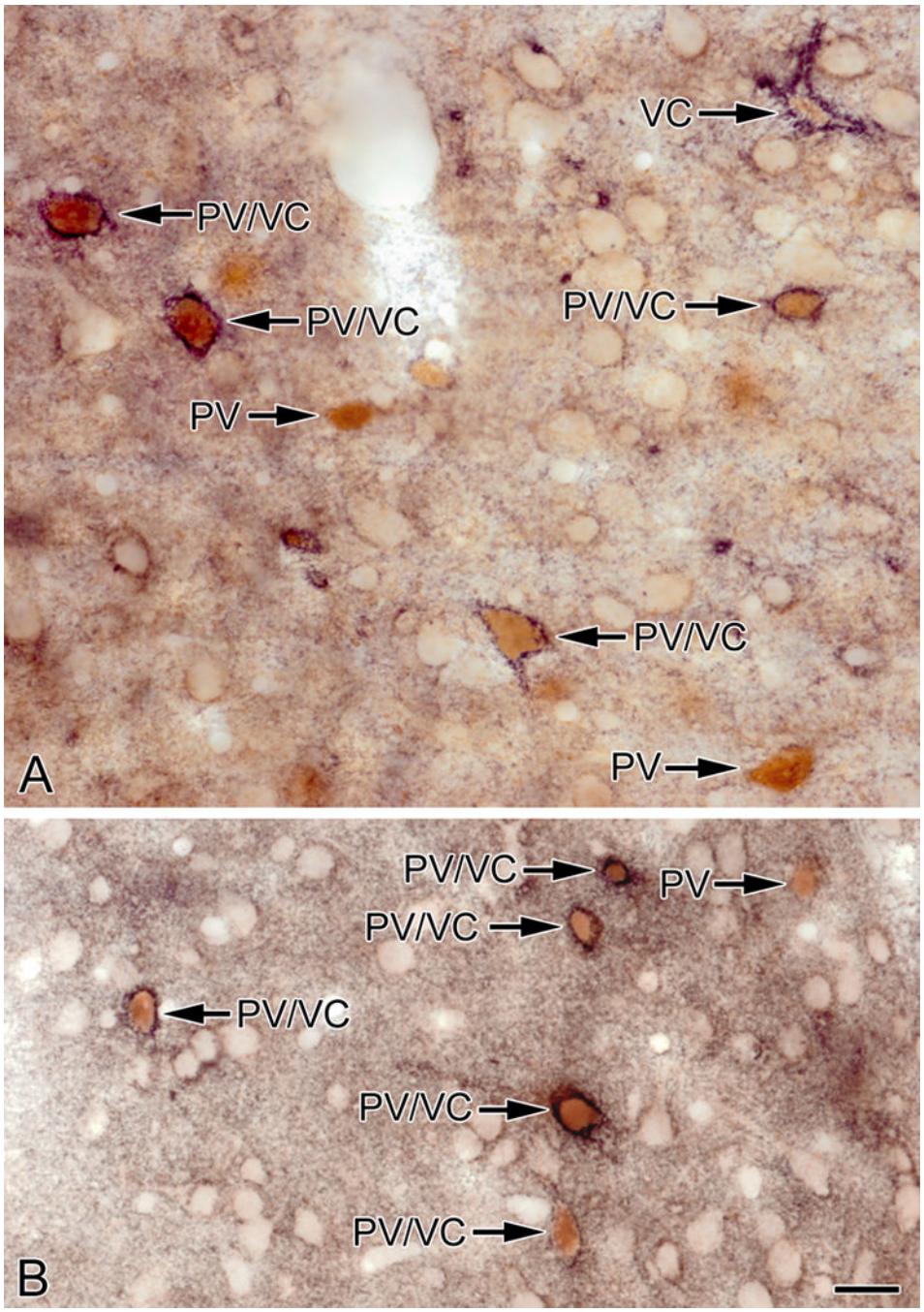

Fig. 7.

Photomicrographs of sections through the BLa (A) and lateral nucleus (B) stained for VC1.1 (black) and PV (brown). Most PV+ neurons are ensheathed by VC1.1+ PNNs (PV/VC) but some are not (PV). One neuron in A is ensheathed by a VC1.1+ PNN but exhibits little or no PV immunoreactivity (VC). *Scale bar = 20 μm for both A and B*

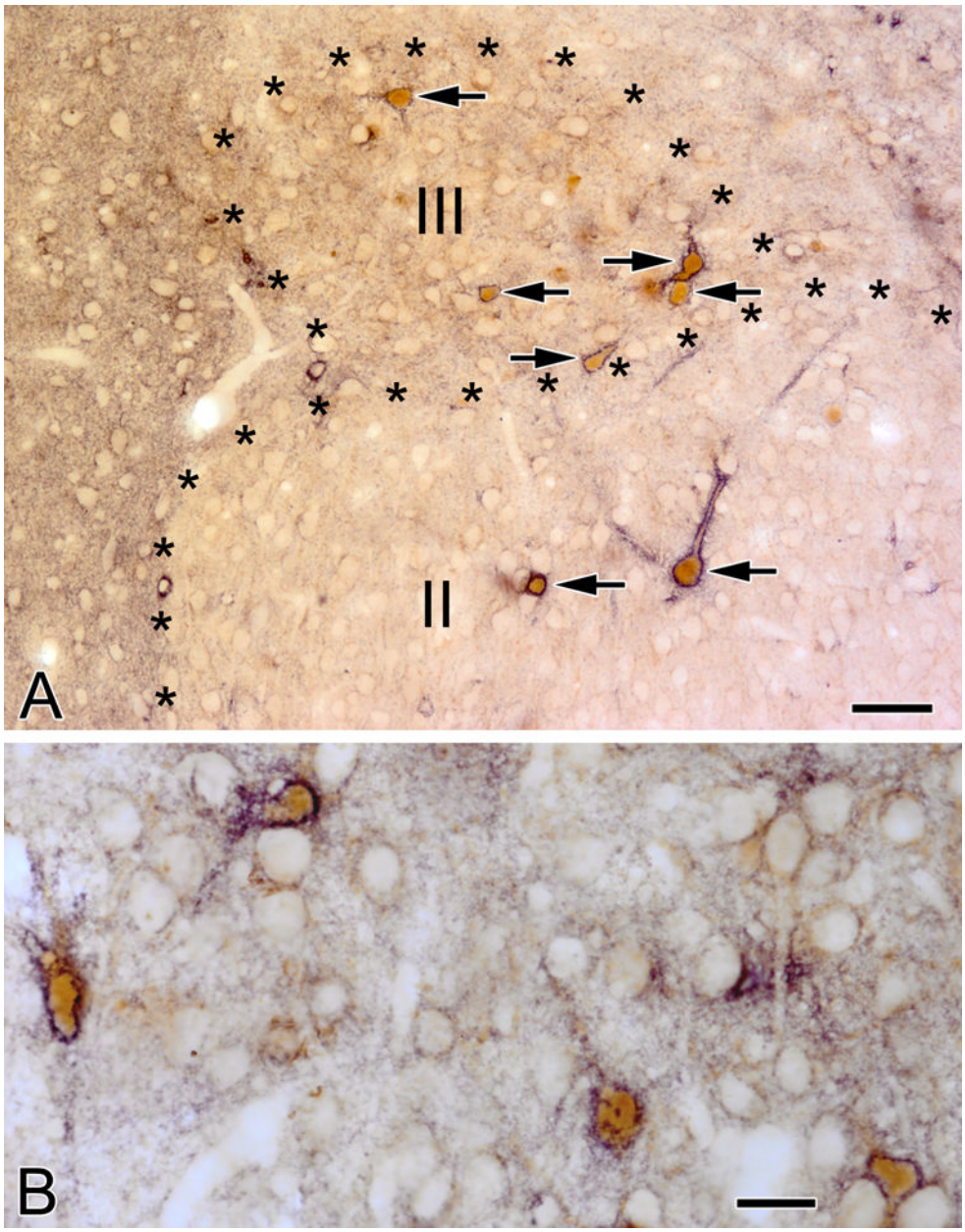

Fig. 8.

(A) VC1.1+ PNNs (black) surround PV+ neurons (brown) in the nucleus of the lateral olfactory tract. Two of these neurons are in layer II and five are in layer III (arrows). (B) Four PV+ neurons (brown) in the amygdalohippocampal area are ensheathed by VC1.1+ PNNs (black). *Scale bar = 50 μm in A and 20 μm in B*

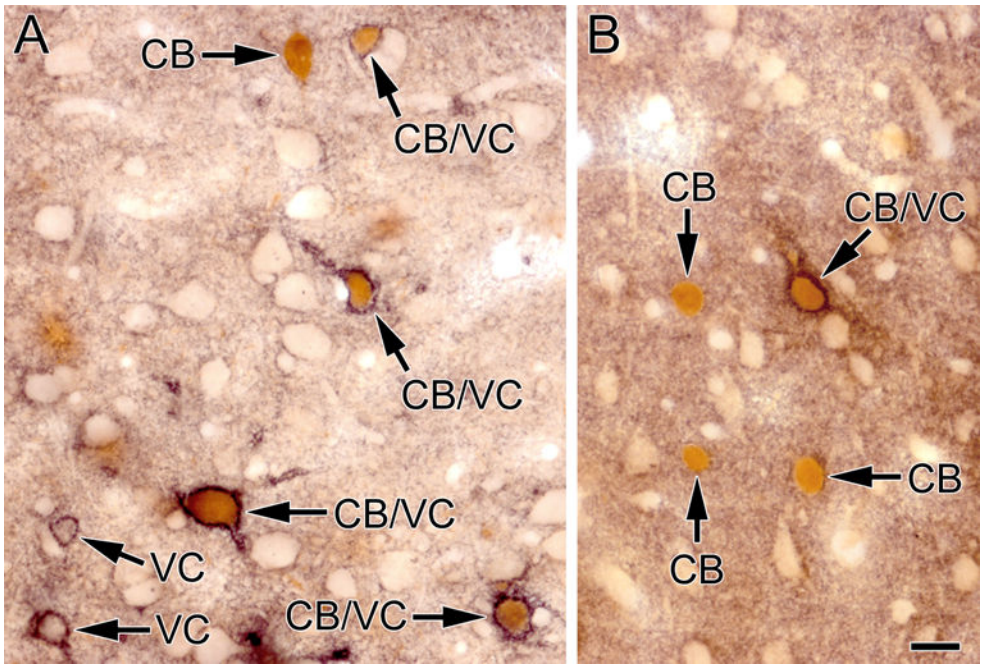

Fig. 9.

Photomicrographs of sections through the BLa (A) and lateral nucleus (B) stained for VC1.1 (black) and CB (brown). Several CB+ neurons are ensheathed by VC1.1+ PNNs (CB/VC) but some are not (CB). Two neurons in A are ensheathed by a VC1.1+ PNN but exhibit no CB immunoreactivity (VC). *Scale bar = 20 μm for both A and B*

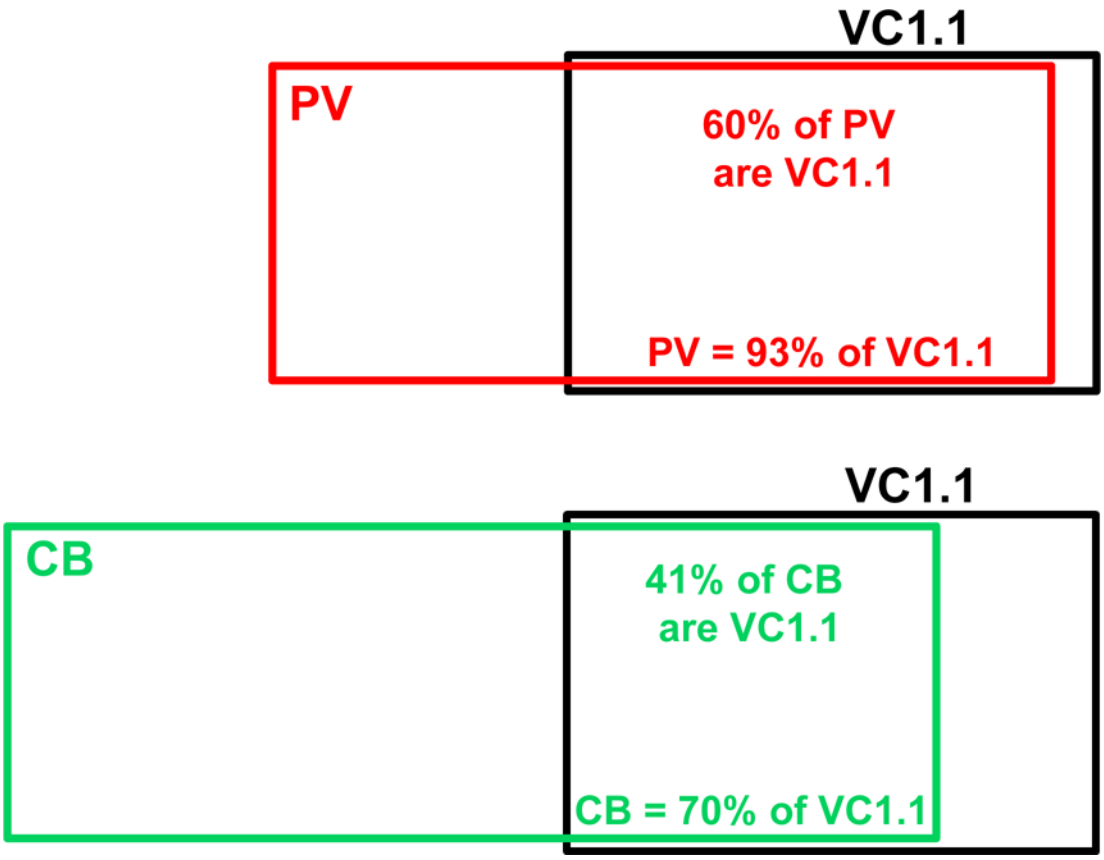

Fig. 10.

Venn diagrams illustrating the relationship of PV+ neurons (upper diagram) and CB+ neurons (lower diagram) to VC1.1+ neurons in the BLa. The sizes of the rectangles indicate the relative numbers of the different neuronal populations. Note that CB+ neurons outnumber PV+ neurons in the BLa. Approximately 80% of PV+ neurons are CB+, and these PV+/CB+ neurons constitute about 60% of the CB+ population (McDonald and Betette, 2001)

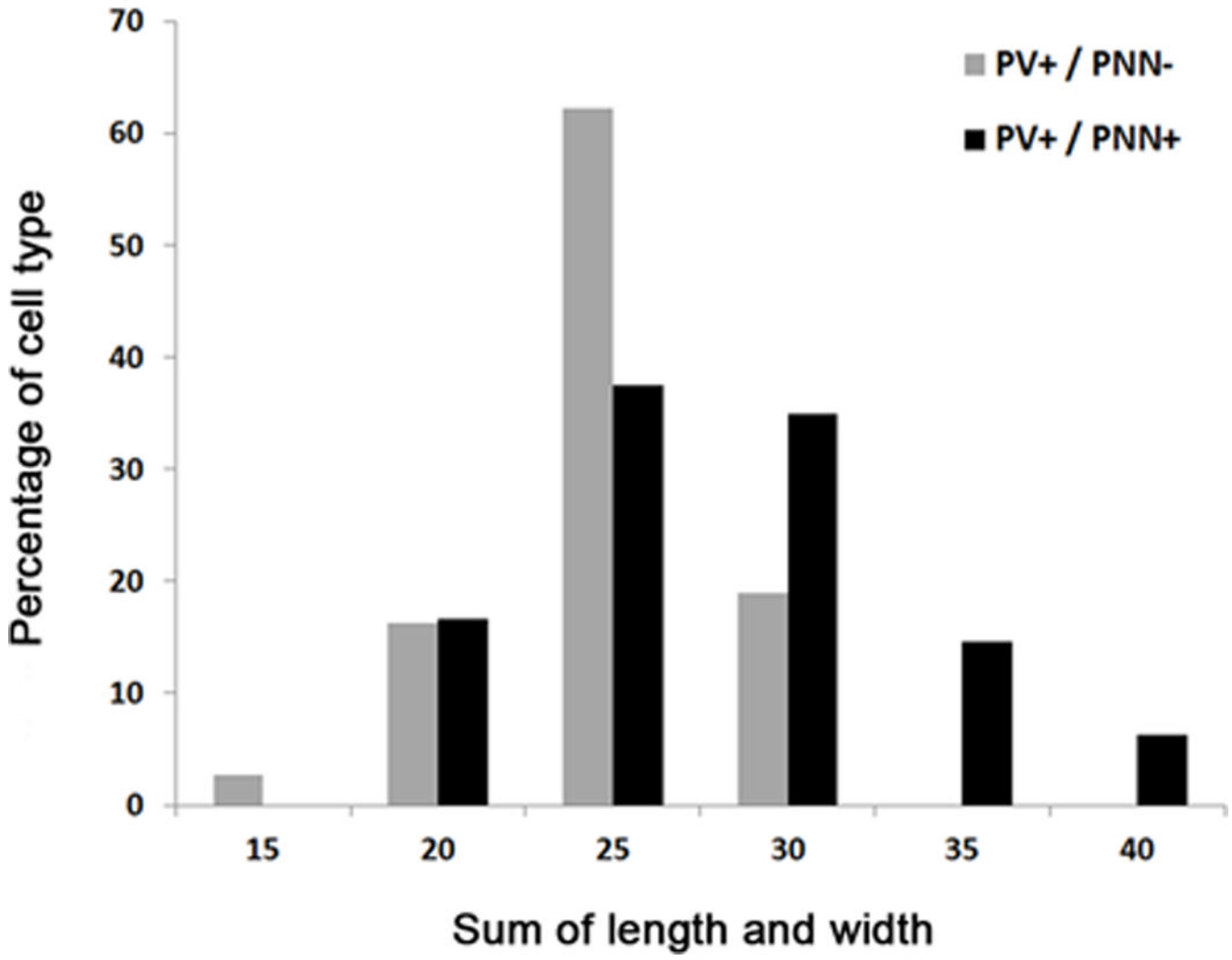

Fig. 11.

Histogram showing the perikaryal sizes of PV+ interneurons ensheathed by VC1.1+ PNNs (PV+/PNN+; black) and PV+ interneurons not ensheathed by VC1.1+ PNNs (PV+/PNN–; gray) in the BLa

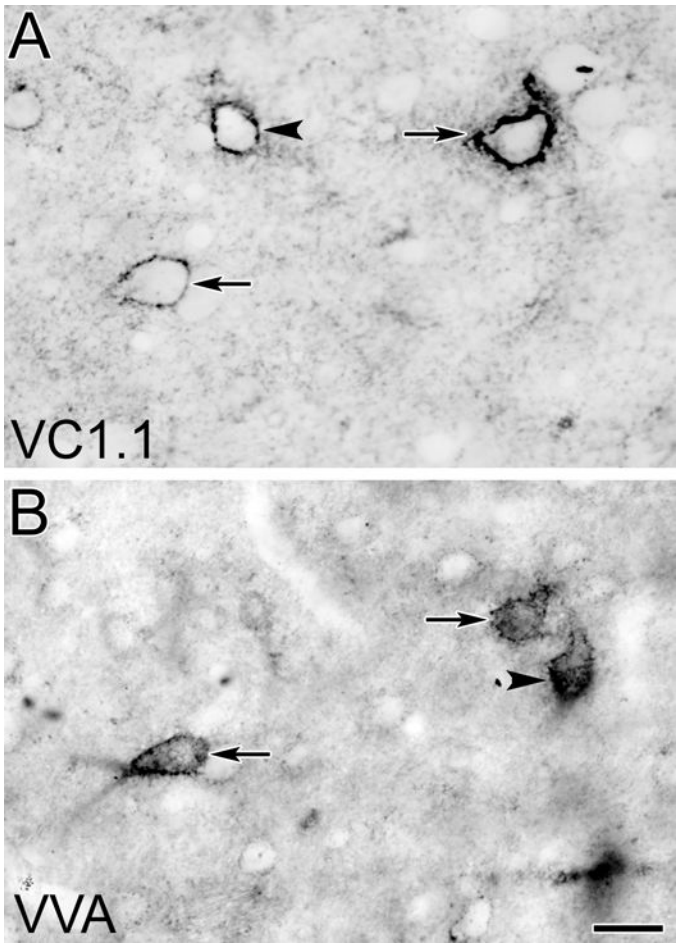

Fig. 12.

Photomicrographs of corresponding surfaces of adjacent sections through the BLa stained with the VC1.1 antibody (A) or VVA (B). Arrows indicate two VC1.1+/VVA+ neurons that were stained in both sections. Arrowhead in A indicates a single-labeled VC1.1+ neuron. Arrowhead in B indicates a single-labeled VVA+ neuron. *Scale bar = 20 μm for both A and B*

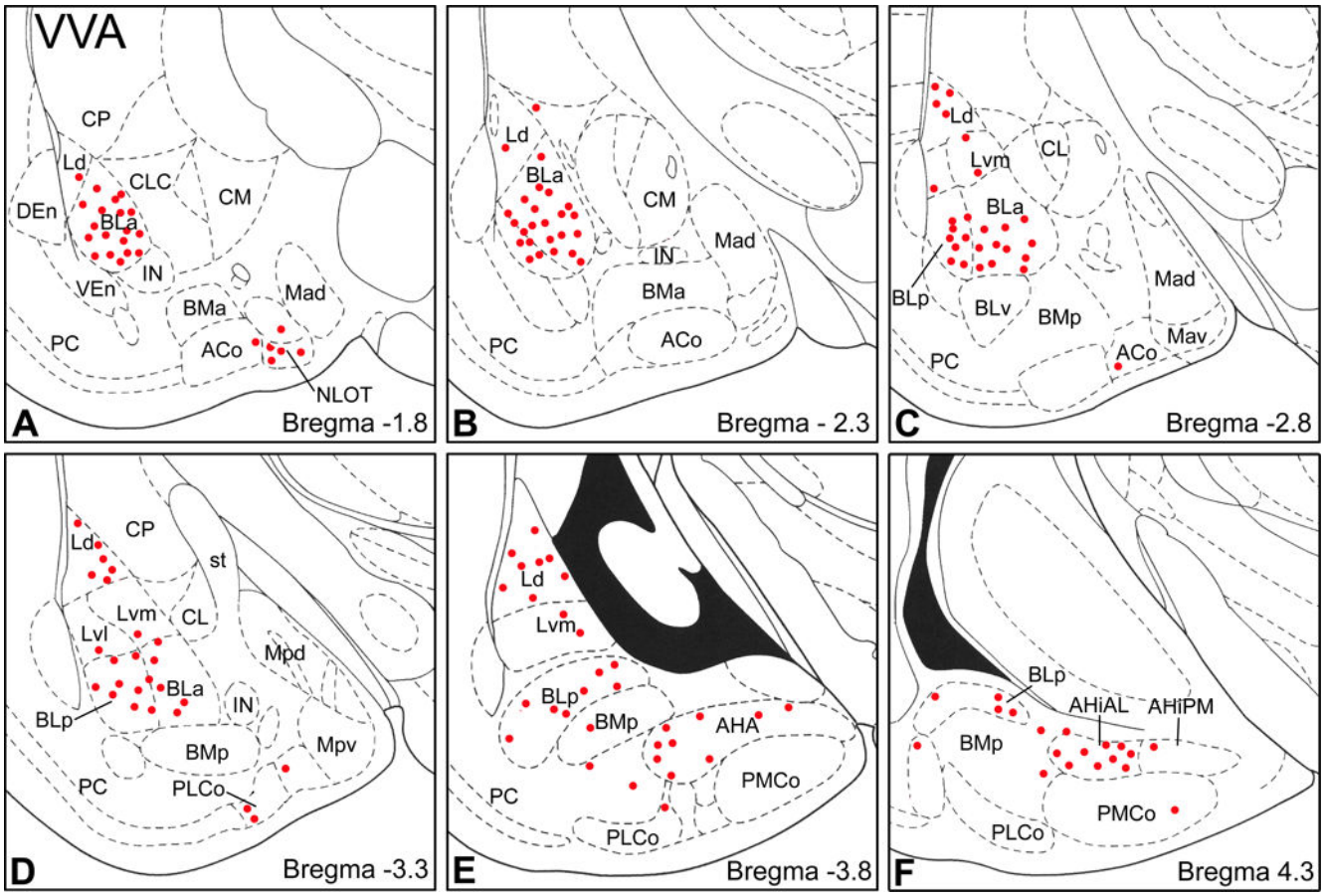

Fig. 13.

Distribution of VVA+ PNNs in the amygdala (red dots) in sections arranged from rostral (A) to caudal (F). Each bregma level shows the locations of neurons plotted from three non-adjacent 50 μm-thick sections; each dot represents one neuron. Templates are modified from the atlas by Paxinos and Watson (1997). For abbreviations see caption for Figure 2.

Table 1

Association of VC1.1+ perineuronal nets with PV+ neurons in the anterior subdivision of the basolateral nucleus (BLa). Counts in the BLa of each of these three types of neurons were made in a total of 7-10 amygdalar sections from each brain (from both left and right sides; bregma levels −1.7 to −3.0).

Brain	Single-labeled PV+ neurons	Single-labeled VC1.1+ neurons	Double-labeled PV+/VC1.1+ neurons	% of PV+ neurons that were VC1.1+	% of VC1.1+ neurons that were PV+
VC-11	51	2	71	58.2% (71/122)	97.3% (71/73)
VC-18	56	7	83	59.6% (83/139)	92.2% (83/90)
VC-23	52	9	93	64.1% (93/145)	91.1% (93/102)
Total	159	18	247	60.8% (247/406)	93.2% (247/265)

Table 2

Association of VC1.1+ perineuronal nets with CB+ neurons in the anterior subdivision of the basolateral nucleus (BLa). Counts in the BLa of each of these three types of neurons were made in a total of 8-9 amygdalar sections from each brain (from both left and right sides; bregma levels −1.7 to −3.0).

Brain	Single-labeled CB+ neurons	Single-labeled VC1.1+ neurons	Double-labeled CB+/VC1.1+ neurons	% of CB+ neurons that were VC1.1+	% of VC1.1+ neurons that were CB+
VC-11	66	12	46	41.1% (46/112)	79.3% (46/58)
VC-18	64	28	48	42.9% (48/112)	63.2% (48/76)
VC-23	61	16	41	40.2% (41/102)	71.9% (41/57)
Total	191	56	135	41.4% (135/326)	70.7% (135/191)

Table 3

Colocalization of VC1.1+ and VVA+ perineuronal nets in the anterior subdivision of the basolateral nucleus (BLa). Counts in the BLa of each of these three types of neurons were made in a total of 6-7 amygdalae from each brain (from both left and right sides; bregma levels −1.7 to −3.0).

Brain	Single-labeled VVA+ neurons	Single-labeled VC1.1+ neurons	Double-labeled VC1.1+/VVA+ neurons	% of VVA+ neurons that were VC1.1+	% of VC1.1+ neurons that were VVA+
VC-22	18	8	25	58.1% (25/43)	75.8% (25/33)
VC-17	14	6	23	62.2% (23/37)	79.3% (23/29)
Total	32	14	48	60.0% (48/80)	77.4% (48/62)